Nonlinear Moving Horizon Observers: Theory & Real-Time Implementation

Mazen Alamir[1]

Centre National de la Recherche Scientifique (CNRS).
GIPSA-Lab. Control Systems Department. SysCo-Team
BP 46, Rue de la Houille Blanche,
Domaine Universitaire, 38400 Saint Martin d'Hères, France.
mazen.alamir@inpg.fr

1 Definitions & Notation

In this chapter, the concept of Moving-Horizon Observer (**MHO**) is recalled and some related topics are discussed and illustrated through dedicated examples. Throughout this chapter, interest is focused on nonlinear systems that may be described by the following equations:

$$x(t) = X(t, t_0, x_0), \tag{1}$$
$$y(t) = h(t, x(t)), \tag{2}$$

where $X : \mathbb{R}_+ \times \mathbb{R}_+ \times \mathbb{R}^n \to \mathbb{R}^n$ is a map that gives the state $x(t)$ of the system at instant t based on the knowledge of the state $x(t_0) = x_0$ at some instant t_0. The map $X(\cdot, \cdot, \cdot)$ may be obtained by using an appropriate system model (Ordinary Differential Equations (ODE's), Differential Algebraic Equations (DAE's) or even a quite sophisticated hybrid simulator). Some of the results presented hereafter may need a particular system model. This is indicated when needed. $y(t) \in \mathbb{R}^{n_y}$ denotes the measured output at instant t. Using similar notations as for the state, the output trajectory is denoted hereafter by:

$$Y(\cdot, t_0, x_0) \doteq h(X(\cdot, t_0, x_0)) \tag{3}$$

Note also that in (1)-(2), dependency w.r.t measured variables such as control input, time varying parameters with known time evolution is implicitly handled through the argument t of the map X. When unmeasured disturbances $w \in \mathbb{R}^{n_w}$ and measurement noise $v \in \mathbb{R}^{n_y}$ are to be considered, equations (1)-(2) are replaced by the following ones:

$$x(t) = X(t, t_0, x_0, w_{t_0}^t), \tag{4}$$
$$y(t) = h(t, x(t)) + v(t), \tag{5}$$

where $w_{t_0}^t$ denotes the disturbance profile $\{w(\tau)\}_{\tau\in[t_0,t]}$. Note that these disturbances may also represent model discrepancies. The same notation $v_{t_0}^t$ are used to denote measurement noise profiles.

In the present chapter, it is assumed that some knowledge is available on the admissible sets of states, disturbances and measurement noise. Namely, there are known compact sets maps $\mathbb{X}(\cdot)$, $\mathbb{W}(\cdot)$ and $\mathbb{V}(\cdot)$ such that the following inclusions hold at each instant t:

$$x(t) \in \mathbb{X}(t) \subset \mathbb{R}^n \quad ; \quad w(t) \in \mathbb{W}(t) \subset \mathbb{R}^{n_w} \quad ; \quad v(t) \in \mathbb{V}(t) \subset \mathbb{R}^{n_y}. \tag{6}$$

These constraints enable the following definition to be stated:

Definition 1 (Measurements-compatible configurations).
Consider some time interval $[t-T,t]$ and a corresponding measurement profile y_{t-T}^t. A pair $(\xi,\mathbf{w}) \in \mathbb{X}(t-T) \times [\mathbb{R}^{n_w}]^{[t-T,T]}$ is said to be (y_{t-T}^t)-compatible if the following conditions hold for all $\sigma \in [t-T,t]$:

1. $w(\sigma) \in \mathbb{W}(\sigma)$,
2. $X(\sigma, t-T, \xi, \mathbf{w}) \in \mathbb{X}(\sigma)$,
3. $y_{t-T}^t(\sigma) - Y(\sigma, t-T, \xi, \mathbf{w}) \in \mathbb{V}(\sigma)$.

When these conditions hold, the following short notation is used:

$$(\xi,\mathbf{w}) \in \mathbb{C}(t, y_{t-T}^t) \tag{7}$$

to denote the set of (y_{t-T}^t)-compatible pairs. ♡

Roughly speaking, a (y_{t-T}^t)-compatible pair $(\xi,\mathbf{w})$ is a pair of initial state (at instant $t-T$) and a disturbance profile $\mathbf{w}$ defined on $[t-T,t]$ such that the resulting trajectory obtained by (4) meets the constraints (6) over $[t-T,t]$.

1.1 Technical definitions

In this section, some technical definitions that are needed in the remainder of this chapter are successively given:

- ✓ A function $\alpha : \mathbb{R}_+ \to \mathbb{R}_+$ is a **K-function** if it is positive definite, continuous, strictly monotonic increasing and proper ($\lim_{x\to\infty} \alpha(x) = \infty$).

- ✓ Given some closed subset $\mathbb{S}$ of an Euclidian space $\mathbb{E}$, the projection map $P_{\mathbb{S}}$ is defined as follows:

$$P_{\mathbb{S}} : \mathbb{E} \to \mathbb{S} : P_{\mathbb{S}}(e) = \min_{\sigma\in\mathbb{S}} d(e-\sigma) \tag{8}$$

  where d is some distance that is to be understood from the context.
- ✓ For all matrix A, $\underline{\sigma}(A)$ denotes the smallest singular value of A.

✓ Given a piece-wise continuous function $g(\cdot)$ defined over some time interval I and some integer i, the following notations are used:

$$\|g(\cdot)\|_{L_i} = \int_I \|g(\tau)\|^i d\tau \quad ; \quad \|g(\cdot)\|_\infty = \sup_{\tau \in I} \|g(\tau)\|$$

✓ Given a multi-variable function $f(x_1, x_2, \dots)$, the partial derivative of G w.r.t x_i is shortly denoted by $f_{x_i}(x_1, x_2, \dots)$.

2 The constrained observation problem

Based on the above definitions, the observation problem can be stated as follows:

Definition 2 (The finite horizon observation problem).
The finite horizon observation problem amounts to choose some observation horizon length $T > 0$ and to use at each instant t, the available information, namely:

1. *the system equations (4)-(5)*
2. *the past measurements y_{t-T}^t,*
3. *the constraints (6) and*
4. *some additional exogenous knowledge.*

in order to produce an estimation $\hat{x}(t)$ of the current state $x(t)$. ♡

The need for some *additional Knowledge* comes from the fact that the first three available information (system equations, measurements and constraints) are of no help to choose between all the candidate states that belong to the following subset:

$$\Omega_t = \Big\{ X(t, t-T, \xi, \mathbf{w}) \quad | \quad (\xi, \mathbf{w}) \in \mathbb{C}(t, y_{t-T}^t) \Big\}. \tag{9}$$

Indeed, all states in Ω_t belong to trajectories that respect the constraints and the noise level and are therefore equally valuable candidates to *explain* the output measurements. Therefore, there is indeterminism unless one of the following conditions holds:

✓ $\Omega_t = \{x(t)\}$ or
✓ some additional criteria is considered.

The first case $\Omega_t = \{x(t)\}$ occurs in particular when no disturbances nor measurement noises are present ($\mathbb{W} = \{0\}$ and $\mathbb{V} = \{0\}$) provided that the system is observable in the following trivial sense:

Definition 3 (Uniform Observability of nominal systems).
The system (1)-(2) is uniformly observable if there is some $T > 0$ and a **K-function** *α such that the following inequality holds:*

$$\int_{t-T}^{t} \|Y(\sigma, t-T, x^{(1)}) - Y(\sigma, t-T, x^{(2)})\|^2 d\sigma \geq \alpha(\|x^{(1)} - x^{(2)}\|) \quad (10)$$

for all $t \geq 0$ *and all* $(x^{(1)}, x^{(2)}) \in \mathbb{X}(t-T) \times \mathbb{X}(t-T)$. ♡

Indeed, under disturbance and noise free assumption and for uniformly observable nominal systems, if $X(t, t-T, \xi)$ belongs to Ω_t for some ξ [see (9)], then one has according to condition 3 of definition 1: $y^t_{t-T}(\sigma) = Y(\sigma, t-T, x(t-T)) = Y(\sigma, t-T, \xi)$ for all $\sigma \in [t-T, t]$ and this implies according to (10) that $\alpha(\|x(t-T) - \xi\|) = 0$ which simply means by definition of α that $\xi = x(t-T)$. Consequently, under the above assumptions, the only element in Ω_t is $X(t, t-T, x(t-T)) = x(t)$.

It is important to underline that definition 3 involves state constraints since inequality (10) has to be satisfied only on the set $\mathbb{X}(t-T) \times \mathbb{X}(t-T)$ of admissible pairs. The following example shows a system that is uniformly observable on some restricted region of admissible states but not in the whole state space.

Example 1. Consider the nominal nonlinear system given by:

$$\dot{x}_1 = -x_1 + x_2 \quad ; \quad \dot{x}_2 = 0 \quad ; \quad y = x_1 x_2$$

This system is observable on the subset $\mathbb{X} = \{x \in \mathbb{R}^2 \mid x_2 > 0\}$ but not on $\mathbb{R}^2$. This is because any pair of states $(x^{(1)}, x^{(2)})$ such that $x^{(1)} = -x^{(2)}$ leads to identically the same output profile. This would contradict (10) if *global* uniform observability is checked. ♢

In the general uncertain and noisy situations, Ω_t may not be a singleton and one needs to add some additional requirement in order to *make the best choice* between all the pairs $(\xi, \mathbf{w}) \in \mathbb{C}(t, y^t_{t-T})$. Once such a criterion is defined, the *best choice* denoted by $(\hat{\xi}(t), \hat{\mathbf{w}}(t))$ is used to compute the best state estimate $\hat{x}(t)$ according to:

$$\hat{x}(t) = X(t, t-T, \hat{\xi}(t), \hat{\mathbf{w}}(t)) \quad (11)$$

Typically, one way to define a choice criterion is to look for $(\xi, \mathbf{w}) \in \mathbb{C}, (t, y^t_{t-T})$ that minimizes some functional:

$$J(t, \xi, \mathbf{w}) := \Gamma(t, \xi - \xi^*(t)) + \int_{t-T}^{t} L\Big(\mathbf{w}(\sigma), \varepsilon_y(\sigma)\Big) \quad \text{where} \quad (12)$$

$$\varepsilon_y(\sigma) \; = \; y^t_{t-T}(\sigma) - Y(\sigma, t-T, \xi, \mathbf{w}). \quad (13)$$

More precisely, the *best choice* $(\hat{\xi}(t), \hat{\mathbf{w}}(t))$ is obtained by solving the following optimization problem:

$$P(t) \quad : \quad \min_{(\xi, \mathbf{w}) \in \Omega_t} J(t, \xi, \mathbf{w}) \quad (14)$$

Note that the definition of the performance index J introduces an *additional knowledge* through the relative weights on the disturbance term w and the output prediction error term ε_y. The resulting trade-off recalls the one introduced in the Kalman filter by using penalties equal to the inverses of the corresponding covariance matrices, namely:

$$L(w, \varepsilon_y) = w^T Q^{-1} w + \varepsilon_y^T R^{-1} \varepsilon_y$$

Moreover, the weighting term $\Gamma(\cdot, \cdot)$ in (12) enables to penalize the distance between ξ and some particular value $\xi^*(t)$ that may condense the past knowledge on the most likely value of the state at instant $t - T$. The value of $\xi^*(t)$ is generally induced by the *past estimation*.

Remark 1. The formulation given above can be viewed as the generalization of the Kalman filter equations that hold only for linear unconstrained systems with particular statistical properties of the uncertainty (w) and the measurement noise v (white Gaussian signals). In this case, the penalty term writes $\Gamma(t, \eta) = \eta P(t) \eta$ and $\xi^*(t)$ is induced by the past estimation giving rise to the Kalman filter updating rules in the discrete or in the continuous case (see [3] for more details).

2.1 About temporal parametrization of uncertainties

In this section, attention is focused on the need for temporal parametrization of uncertainties when using (11)-(14) to design a nonlinear observer. Indeed, the decision variable $(\xi, \mathbf{w})$ involved in the optimization problem $P(t)$ is infinite dimensional as $\mathbf{w}$ is the uncertainty profile over the time interval $[t-T, t]$. Consequently, any concrete implementation of the above scheme needs a finite dimensional approximation of candidate profiles $\mathbf{w}$.

In many academic texts (see for instance [3]), a discrete time version of the system model is used and a piece-wise constant structure is implicitly used with the unknowns

$$p_w := \{\mathbf{w}(k\tau)\}_{k=k_0}^{k_0+N-1} \in \mathbb{W}(k_0) \times \cdots \times \mathbb{W}(k_0 + N - 1) \subset \mathbb{R}^{n_w \cdot N},$$

where $\mathbb{W}(k)$ is a short writing of $\mathbb{W}(k\tau)$ and where the observation horizon length is $T = N\tau$. This leads to a decision variable (ξ, p_w) of dimension $n + N \cdot n_w$.

This choice although apparently natural shows the following major drawbacks:

1. First, the piece-wise constant structure is very often too rich when compared to realistic uncertainties that are often due to badly identified rather constant parameters, slowly drifting variables or even periodic disturbances. This excess of spectral content enlarges the *size* of the set Ω_t of candidate paires [see (9)] and hence lead to noisy estimation even in

presence of small physical measurement noise.

2. In addition to the drawback mentioned above, the piecewise constant structure leads to a high dimensional decision variable $(n + N \cdot n_w)$ with a generally badly conditioned optimization problem. This is because the high spectral content of the resulting $\mathbf{w}$ leads to too many possible *interpretations* of the past measurements.

3. In case of continuously varying uncertain signals, the piecewise constant parametrization implies a small sampling time leading again to even higher dimensional problem for the same observation horizon (buffer length).

One way to overcome these drawbacks is to choose a parametrization of $\mathbf{w}$ that reflects in a more realistic way what would be the time evolution of this uncertainty vector. This can be denoted generically by:

$$w(t) = \mathcal{W}(t, p_w) \quad ; \quad p_w \in \mathbb{P}.$$

Note that here, the dimension of the unknown disturbance parameter p_w is no more directly related to the dimension of the disturbance vector w nor to the length of the observation horizon. The cost function to be minimized can then be rewritten as a function of the new decision variable (ξ, p_w):

$$J(t, \xi, p_w) = J(t, \xi, \mathcal{W}(\cdot, p_w)). \tag{15}$$

Example 2. A typical example of reduced dimensional parametrization of an uncertainty vector that evolves smoothly in time is to use time polynomial approximations:

$$\mathcal{W}_i\big(t, (\underbrace{p_w^{(1)}, \ldots, p_w^{(n_w)}}_{p_w})\big) = P_{\mathbb{W}(t)}\Big[(1, t, \ldots, t^{n_w^{(i)}}) \cdot p_w^{(i)}\Big] \quad ; \quad p_w^{(i)} \in \mathbb{R}^{n_w^{(i)}}. \tag{16}$$

where $P_{\mathbb{W}(t)}(\cdot)$ is the projection map on the admissible set $\mathbb{W}(t)$.

The order of the polynomial development for the i-th component of p_w, namely $n_w^{(i)}$ is to be chosen according to what could be a realistic evolution of this component during the observation horizon $[t-T, t]$. The resulting optimization problem shows a decision variable (ξ, p_w) of dimension

$$n_p := n + \sum_{i=1}^{n_w} n_w^{(i)}.$$

It goes without saying that other time parameterizations can be used in order to be closer to any available information about the uncertainty evolution. $\diamondsuit$

When such parametrization is used, the following straightforward notation is adopted to denote the corresponding state trajectory:

$$X(t, t_0, x_0, p_w) = X\big(t, t_0, x_0, \mathcal{W}(\cdot, p_w)\big).$$

The *best* estimate of the state is then given by

$$\hat{x}(t) = X(t, t - T, \hat{\xi}(t), \hat{p}_w(t))$$

where the pair $(\hat{\xi}(t), \hat{p}_w(t))$ minimizes the cost function $J(t, \xi, p_w)$ defined by (15).

Note that by using the extended state:

$$\bar{x} = \left(x^T \; p_w^T\right)^T \in \mathbb{R}^n \times \mathbb{R}^{n_p}, \tag{17}$$

together with the trivial dynamic $\dot{p}_w = 0$ on the *additional state* vector, the uncertain observation problem is put in a deterministic uncertainty free context with a higher dimensional extended system. Note however that for the new extended uncertainty-free system, the admissible set Ω_t is generally not reduced to $\{x(t)\}$ and the result is still dependent on the additional knowledge that are introduced through the weighting parameters of the cost function $J(t, \xi, p_w)$.

Heuristic approaches can also be used to avoid time structured model of the uncertainties evolution that are not discussed here. See [13] for more details.

2.2 Optimization based vs analytic observers

Recall that the Kalman filter equations are originally derived based on optimal design considerations (maximum likelihood under white Gaussian signals assumption). One nice feature of the observer equations is that in the absence of disturbances and measurement noise, the estimation error:

$$e := x - \hat{x}$$

shows a comprehensively asymptotically stable dynamic behavior with a stable closed loop matrix. The generalization of the optimization based formulation that underlines the Kalman filter to general nonlinear systems leads to generally non convex and hard to solve optimization problems.

This fact together with the relatively limited computational facilities in the 80's motivated researches on nonlinear observers that are based on the study of the resulting estimation error's dynamic and that can be expressed in analytic form without the use of on-line computations. However, the possibility to derive observer equations such that the induced dynamics on the estimation

error is *provably asymptotically stable* is quite limited. Indeed, given a general nonlinear system expressed in ODE's form

$$\dot{x} = f(x) \quad ; \quad y = h(x), \tag{18}$$

and a candidate consistent observer equation:

$$\dot{\hat{x}} = f(\hat{x}) + K(\hat{x}, y)$$

the explicit observer design problem amounts to find a function $K(\cdot,\cdot)$ of the observer's internal state and the measured output such that the induced estimation error equation that is involved in the extended resulting ODE's:

$$\begin{aligned} \dot{x} &= f(x) \\ \dot{e} &= f(x) - f(x-e) - K(h(x), x-e) \end{aligned}$$

can be proved to be asymptotically stable. This is clearly a hard task as long as a high level of genericity is required.

To overcome this difficulty, researchers imagined conditions on the maps f and h involved in the system and measurement equations (18) in order for a correction map $K(\cdot,\cdot)$ to be found. High gain observers [20, 2] and sliding mode observers [4, 10, 23] resulted from this approach.

Almost twenty years of this *state estimation error* (**SEE**)-based observer design enforced the idea according to which, the very basic notion of observability expressed in definition 3 is largely insufficient to derive a concrete state estimation scheme. Additional (generally structural) properties are still needed in order for a state observer to exist. Moreover, these additional conditions are constructive in the sense that they are needed not only to guarantee the convergence of the estimation error but they are needed for the observer design itself.

It goes without saying that, faced with these difficulties even in the nominal case, studies on nonlinear observers were essentially directed towards nominal state estimation problems (without uncertainty nor measurement noises). The robustness issues are generally viewed as a by-side product or tackled through an even more restrictive structural properties that are expressed for some extended systems in the spirit of what is presented in section 2.1.

Contrary to analytic observers that use the explicit study of the state estimation error in order to design the observer correction term, optimization based observers use the very definition of observability in order to derive the state estimation algorithm. The idea is to use the fact that as long as the nominal system is considered, estimating the state of an observable system is equivalent to minimizing $J(t,\xi)$: the integral of the squared output prediction

error over some observation horizon (see definition 3).

Consequently, if an algorithm can guarantee that this quantity converges asymptotically to 0, then there is no need for additional proof of convergence. The convergence of the state estimation error is a direct consequence of the convergence of the cost function $J(t, \xi(t))$ since this proves that $\xi(t)$ converges to $x(t-T)$ and that $\hat{x}(t) = X(t, t-T, \xi(t))$ converges to $x(t)$.

Unfortunately, there is no such algorithms with guaranteed convergence properties for general non convex optimization problems. The keywords *Global convergence* that is widely used in scientific papers refer to global convergence to *some local minimum*. Convergence results still need dedicated sufficient conditions. However, these sufficient conditions are not constructive unlike the ones used in analytic observers design. These conditions are not needed in the construction of optimization based state estimation algorithms. More clearly, even if one cannot guarantee the convergence of the resulting state estimation scheme, one can always *investigate* the performance of an optimization based observer on his own system. It is likely that the resulting scheme works quite correctly even so there is no convergence proof.

Another difficulty arises when using optimization based nonlinear observer. This concerns the real-time implementability issue. Indeed, the number of iterations that would be needed for a solver to *find* the optimal solution of $P(t)$ may exceed the available computation time that would be compatible with the necessary updating rate. This difficulty is made worst by the fact that each evaluation of the cost function needs the evolution of the system to be *simulated* during the observation horizon which may be heavy to perform.

In a word, optimization based nonlinear observers offer several advantages such as constraints handling and independence w.r.t the mathematical model of the system. However, there are still several bottlenecks in their implementation and reliability. Despite these difficulties, these observers are very often the only available choice. Consequently, investigating implementation issues that enable to (at least partially) overcome the above mentioned difficulties is certainly a *profitable investment*. This is the aim of this chapter.

Typically, two main issues are to be considered when implementing moving-horizon observers:

- The first one is related to the presence of local valleys that may attract the optimization process leading to bad estimation of the state. As long as generic observer design is concerned, this problem is unavoidable in constrained non convex optimization. However, one can use a very particular feature of the state estimation induced optimization problem to derive singularities avoidance heuristic scheme. This is depicted in section 3 with an

experimental validation on a terpolymerization processes.

- The second implementation issue is related to the computation time the iterative process would need to achieve the optimization task. This time may be prohibitive when compared to the necessary updating rate. In this chapter, two different approaches to address this problem are discussed:

  - In the first, a differential formulation of moving horizon observer is proposed. In this formulation, the observer equations take a rather standard form (the observer equations is obtained by copying the system equation and adding a correction term). The only difference is that the correction term uses an integral norm of the output prediction error rather than a point-wise output prediction error. This formulation and the related techniques enabling to reduce the computational burden are discussed in section 4.

  - In the second approach to address the real-time implementation issue, the optimization process is *distributed over the system life-time*. A concrete derivative-free iterative scheme is proposed that may address discontinuous (hybrid) behavior of the dynamic system. This scheme is presented in section 5

As it is discussed in section 2.2, in the forthcoming developments, the robustness issue is addressed indirectly by extending the state vector or by a posteriori validating tests.

3 Singularities Avoidance Heuristic Scheme

In this section, we consider a nominal system given by (1)-(2). The observer design is developed on the nominal system under the uniform observaility assumption (see definition 3). The robustness of the state estimation algorithm is then checked under modeling errors and measurement noise as well as experimentally on a real terpolymerization reactor[1].

3.1 Expression of The Moving Horizon Observer

Using the notations of section 2 in the nominal context, consider a sampled receding-horizon observer with observation horizon $T = N\tau_s$ that updates the estimated state at instants $t_k = k\tau_s$ according to:

[1] The experimental part of this section is a result of a joint work with Nida Sheibat-Othman and Sami Othman for the Laboratoire d'Automatique et du Génie des Procédés (LAGEP, Lyon, France). See [17].

$$\hat{x}(t_k) = X(t_k, t_{k-N}, \hat{\xi}(t_k)) \tag{19}$$

$$\hat{\xi}(t_k) = arg \min_{\xi \in \mathbb{X}(t_{k-N})} \Big[J(t_k, \xi) \Big] := \sum_{i=k-N}^{k} \| y(t_i) - Y(t_i, t_{k-N}, \xi) \|^2_{Q_i(k)} \tag{20}$$

where for all $i \in \{1, \ldots, N\}$, $Q_i(k) \in \mathbb{R}^{n_y \times n_y}$ is a positive definite weighting matrix. Note here that there is no more integrals used to define the cost function as the measurements are assumed to be acquired with the sampling period τ_s.

Reference to uniform observability is therefore implicitly based on a slight adaptation of definition 3 to the case of sampled measurement acquisition. This would lead to what could be referred to as uniform observability under τ_s-sampling. The corresponding definition is identical to definition 3 with the l.h.s of (10) being replaced by the r.h.s of (20)

Recall that under the uniform observability assumption, the optimization problem (20) admits a unique global minimum $\hat{\xi}(t_k) = x(t_{k-N})$. Moreover, this global minimum correspond to à 0 optimal cost value.

The solution of the constrained generally non convex optimization problem (20) is ideally obtained as the asymptotic output of some iterative subroutine $\mathcal{S}$ (see figure 1), namely:

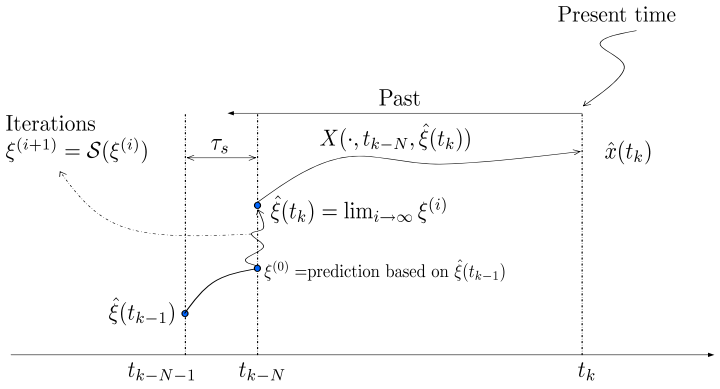

Fig. 1. Ideal computation scheme to solve the optimization problem (20). The iterative process $\mathcal{S}$ is initialized at $\xi^{(0)}$ that is obtained using the past estimated value $\hat{\xi}(t_{k-1})$. Then, the iterations ideally lead asymptotically to the solution $\hat{\xi}(t_k)$. Integrating the system equations enables the computation of the current estimation $\hat{x}(t_k)$.

$$\hat{\xi}(t_k) \leftarrow \lim_{i\to\infty} \xi^{(i)} \tag{21}$$

$$\xi^{(i+1)} = \mathcal{S}(\xi^{(i)}, t_k, y_{t_{k-N}}^{t_k}) \quad ; \quad \xi^{(0)} = X(t_{k-N}, t_{k-N-1}, \hat{\xi}(t_{k-1})) \tag{22}$$

More precisely, an initial guess $\xi^{(0)}$ for the iterative process is computed based on the past estimation $\hat{\xi}(t_{k-1})$ by integrating the system equations one sampling period ahead. The iterations defined by (22) can then be performed to yield $\hat{\xi}(t_k)$ after some iterations and the estimation $\hat{x}(t_k)$ is obtained according to (19).

Note that the initialization of the iterative process by $\xi^{(0)}$ that is based on the past estimation represents in some way an exogenous knowledge that is *injected* in addition to the past measurements. Note also that this can be used explicitly in the definition of the cost function to play the role of ξ^* invoked in section 2. More precisely, one can replace the cost function used in (20) by:

$$J^*(t_k, \xi) := \|\xi - \xi^{(0)}\|_{Q_0} + \sum_{i=k-N}^{k} \|y(t_i) - Y(t_i, t_{k-N}, \xi)\|^2_{Q_i(k)} \tag{23}$$

where $\xi^{(0)}$ is given by (22).

It goes without saying that in practice, the number of iterations of the process $\mathcal{S}$ that can be performed within a sampling period τ_s is necessarily limited and the assignment in (21) must be replaced by:

$$\hat{\xi}(t_k) = \xi^{(N_{max})} = \mathcal{S}^{N_{max}}(\xi^{(0)}, t_k, y_{t_{k-N}}^{t_k}) \tag{24}$$

where $\mathcal{S}^j(\cdot)$ denotes the results of j successive applications of the map $\mathcal{S}$ starting from the initial guess $\xi^{(0)}$. More precisely, the number of iterations depends on the required precision $\varepsilon > 0$ used in the solver and N_{max} is just an upper bound on this number. Consequently, the number of effective iterations $N_{eff}(t_k, \varepsilon) \leq N_{max}$ varies in time with the parameters $x(t_k)$, $y_{t_{k-N}}^{t_k}$ that contribute to the definition of the optimization problem and its related complexity for a given required precision ε. It results that using an a priori given bound N_{max}, the required precision is no more guaranteed even regardless the problem of local minima.

Now, regardless the iterative process $\mathcal{S}$ used to perform the optimization task, local minima may exist that potentially prevent the iterate $\xi^{(i)}$ from converging to the global minimum $x(t_{k-N})$. This is afforded by using multiple initial guesses unless some other characterization of the global minimum is available.

Fortunately, when dealing with the nominal state estimation problem for uniformly observable systems, the global minimum $x(t_{k-N})$ one looks for when trying to solve the optimization problem (20) can be strongly characterized by the following property:

$x(t_{k-N})$ is the unique global minimum of ALL the optimization problems (20) that may be obtained by changing the positive definite weighting matrices $Q_i(k)$.

This makes the state estimation problem a very particular optimization problem since the global minimum one is looking for is THE global minimum of an infinite number of KNOWN functons. A subset of this set of functions sharing $x(t_{k-N})$ as global minimum can be generated by choosing the following family of weighting matrices:

$$Q_i(k) = \gamma^{k-i} \cdot q_i \cdot \mathbb{I}_{n_y} \quad \text{s.t} \quad q_i > 0 \quad \text{and} \quad \sum_i q_i = 1 \tag{25}$$

where $\gamma \in [0, 1]$ is some forgetting factor while $\mathbb{I}_{n_y}$ is the identity matrix in $\mathbb{R}^{n_y \times n_y}$. Note that since the vector of weights:

$$\bar{q} = \begin{pmatrix} q_1 \; q_2 \; \dots \; q_{n_y} \end{pmatrix}^T \tag{26}$$

is involved in the definition of the cost function (20), the iterative process (24) can be worth rewritten in the following form:

$$\hat{\xi}(t_k) = \mathcal{S}_{\bar{q}}^{N_{max}}(\xi^{(0)}, t_k, y_{t_{k-N}}^{t_k}) \tag{27}$$

The idea is then to notice that a local minimum for (20) in which some weighting vector $\bar{q}^{(1)}$ is used may probably not remain a local minimum for another randomly chosen value of the weighting vector $\bar{q}^{(2)}$ since it seems reasonable to admit that only the true global minimum $x(t_{k-N})$ is a singular point for all possible values of the weighting vector $\bar{q}$. Following this intuition, the *one trials* updating rules (27) is replaced by the following *multiple trials* updating rule:

$\bar{q} \leftarrow \dfrac{1}{n_y}\begin{pmatrix} 1 \; 1 \; \dots \; 1 \end{pmatrix}$; $\hat{\xi}(t_k) =\!\leftarrow X(t_{k-N}, t_{k-N-1}, \hat{\xi}(t_{k-1}))$

for $(i = 1 : N_{\text{trials}})$

$\hat{\xi}(t_k) \leftarrow \mathcal{S}_{\bar{q}}^{N_{max}}(\hat{\xi}(t_k), t_k, y_{t_{k-N}}^{t_k})$

Generate randomly new $\bar{q}$ satisfying (26)

end

$\hat{x}(t_k) \leftarrow X(t_k, t_{k-N}, \hat{\xi}(t_k))$

Note that when $N_{\text{trials}} = 1$, the *multiple trials* updating rule defined above gives the classical *one trial* updating rule (27) in which the initial guess ξ^0 is given by (22).

Note that in the algorithm described above, the quantities t_k, $y_{t_{k-N}}^{t_k}$ and $\hat{\xi}(t_{k-1})$ are inputs while the resulting estimated values $\hat{x}(t_k)$ and $\hat{x}(t_k)$ are outputs while $N_{\text{trials}} \in \mathbb{N}$ is a parameter. This can be shortly written as follows:

$$\hat{\xi}(t_k) = \mathcal{A}_{N_{\text{trials}}}\left(\hat{\xi}(t_{k-1}), t_k, y_{t_{k-N}}^{t_k}\right) \tag{28}$$

$$\hat{x}(t_k) = X(t_k, t_{k-N}, \hat{\xi}(t_k)) \tag{29}$$

which clearly defines a dynamic observer with internal state $\hat{\xi}$ that delivers the estimated state $\hat{x}(t_k)$ as output.

It is worth noting that according to the definition of $\mathcal{A}_{N_{\text{trials}}}(\cdot)$, one need to perform $N_{\text{trials}} \times N_{max}$ iteration of the process $\mathcal{S}$. Denoting by τ_{iter} the time needed to perform a single iteration, the following constraint has to be satisfied:

$$N_{trial} \times N_{max} \times \tau_{iter} \leq \tau_s \tag{30}$$

in order for the above moving horizon observer to be real time implementable with τ_s as updating period.

It is worth noting that in the real-time implementability constraint (30), a trade-off is clearly to be found that is probably problem dependent. Examples may be found in which it is worth increasing N_{trials} and reducing N_{max} and vice-versa. On the other hand, the updating period τ_s may be quite larger than the acquisition rate in order to leave time for convergence.

3.2 Application to a Terpolymerization Batch Process

In this section[2], the moving horizon state observer defined in the preceding section is applied to the state estimation of a terpolymerization batch process.

Multimonomer systems are usually used to produce polymeric materials with suitable final properties. Terpolymerization systems usually allow producing high performance materials. In order to control the final polymer properties, such as the polymer composition, it is of high importance to model and monitor such processes. In particular, monitoring the number of each one of the three monomers is a key issue in controlling the final product quality.

In this section, we will be interested in estimating the polymer composition in emulsion terpolymerization. A complete description of the state estimation results presented in this section can be obtained in [17]. Here, only a sketch of the result are given to illustrate the estimation process described above.

While several estimators have been proposed for polymerization processes (see for instance [22, 21, 7] and the references therein), as long as emulsion

[2] The process description given in this section is basically borrowed from [17] and is due to Nida Sheibat-Othman to whom I am deeply indebted for our fruitful and exciting collaborations.

terpolymerization is concerned, only two applications could be found in the literature. In [12], an open loop observer is designed to estimate the polymer composition using calorimetric measurements combined to the process model. In [19], a closed loop high gain observer is proposed to estimate the polymer composition and it has been shown by simulation and experimentally that the system can be observable if the total amounts of monomers are measured. However, because of the model complexity (see below), the design of such a high gain observer and the tuning of its gain in order to cope with the system constraints remains a quite involved task and the high gain observer has been obtained at the price of tremendous simplification of the dynamic model that lead to rather poor estimation performance.

In the remainder of this section, the process model is first described, then simulations as well as experimental validations are discussed.

Process Model

Assuming that monomers are not soluble in the aqueous phase and that the reaction takes place mainly in the polymer particles, the material balances of monomers are given by:

$$\dot{N}_i = Q_i - R_{Pi} \quad i = 1, 2, 3 \tag{31}$$

The reaction rate in the polymer particles R_{Pi} is proportional to the concentration of monomer in the polymer particles ($[M_i^P]$) and the number of moles of radicals in the polymer particles (μ):

$$R_{Pi} = \mu[M_i^P](k_{p1i}P_1^P + k_{p2i}P_2^P + k_{p3i}P_3^P) \tag{32}$$

The time averaged probabilities (P_i^P) that an active chain be of ultimate unit of type i are defined by:

$$P_1^P = \frac{\alpha}{\alpha+\beta+\gamma} \quad ; \quad P_2^P = \frac{\beta}{\alpha+\beta+\gamma} \quad ; \quad P_3^P = 1 - P_1^P - P_2^P \tag{33}$$

where

$$\begin{aligned}
\alpha &= [M_1^P](k_{p21}k_{p31}[M_1^P] + k_{p21}k_{p32}[M_2^P] + k_{p31}k_{p23}[M_3^P]) \\
\beta &= [M_2^P](k_{p12}k_{p31}[M_1^P] + k_{p12}k_{p32}[M_2^P] + k_{p13}k_{p32}[M_3^P]) \\
\gamma &= [M_3^P](k_{p13}k_{p21}[M_1^P] + k_{p21}k_{p23}[M_2^P] + k_{p13}k_{p23}[M_3^P])
\end{aligned}$$

In emulsion polymerization, it is well known that the reaction can be divided into three intervals. In interval I, the polymer particles are produced. Modelling of this interval allows the calculation of the particle size distribution and the average number of radicals per particle which allows to calculate the total

number of moles of radicals in the polymer particles (μ) in (32). This part of the model will not be considered since it adds a lot of complexity to the process model besides the fact that it remains very sensitive to impurities. μ will therefore be considered as a parameter in the process model to be estimated without modelling. It is important to outline that μ can undergo important changes during the reaction since it is affected by the gel effect phenomena.

In interval II, the particle number is supposed to be constant. Polymer particles are saturated with monomer and the excess of monomer is stored in the monomer droplets. During interval III, monomer droplets disappear and all the residual monomer is supposed to be in the polymer particles. Therefore, the concentration of monomer in the polymer particles can be calculated by the following system:

$$[M_i^P] = \begin{cases} \dfrac{(1-\phi_p^p)N_i}{\sum_j \dfrac{N_j MW_j}{\rho_j}}, & \text{(Phase II)} \\ \dfrac{N_i}{\sum_j MW_j(\dfrac{N_j^T - N_j}{\rho_{j,h}} + \dfrac{N_j}{\rho_j})} & \text{(Phase III)} \end{cases} \tag{34}$$

The condition for the existence of monomer droplets and therefore for determining if the reaction is in interval II, is governed by the following equation:

$$N_1\delta_1 + N_2\delta_2 + N_3\delta_3 - \frac{(1-\phi_p^p)}{\phi_p^p}\sigma > 0 \tag{35}$$

where

$$\delta_i = MWi(\frac{1}{\rho_i} + \frac{(1-\phi_p^p)}{\rho_{i,h}\phi_p^p}) \ , \quad i = 1,2,3 \tag{36}$$

and

$$\sigma = \sum_{j=1}^{3} \frac{MW_j N_j^T}{\rho_j, h} \tag{37}$$

The overall monomer conversion that can be measured easily online by calorimetry is defined by:

$$y = \frac{\sum_{i=1}^{3} MW_i(N_i^T - N_i)}{\sum_{j=1}^{3} MW_j N_j^T} \tag{38}$$

Parameters used for the experimental validation of the model are given in table 1 where $k_{pij} = k_{pii}/r_{ij}$. The recipe used for the experimental validation of the observer is given by table 2 [19].

Parameter	Value	Unit
ϕ_p^p	0.4	
MW_1	128.2	(g/mol)
MW_2	100.12	(g/mol)
MW_3	86.09	(g/mol)
ρ_1	0.89	(g/cm^3)
ρ_2	0.94	(g/cm^3)
ρ_3	0.93	(g/cm^3)
$\rho_{1,h}$	1.08	(g/cm^3)
$\rho_{2,h}$	1.15	(g/cm^3)
$\rho_{3,h}$	1.17	(g/cm^3)
k_{p11}	4.5×10^5	$(cm^3/mol/s)$
k_{p22}	1.28×10^6	$(cm^3/mol/s)$
k_{p33}	4.26×10^6	$(cm^3/mol/s)$
r_{12}	0.355	
r_{21}	1.98	
r_{13}	6.635	
r_{31}	0.037	
r_{23}	22.21	
r_{32}	0.07	

Table 1. Parameter values of the terpolymerization of BuA/MMA/VAc (used in the experimental validation)

Component	Charge (g)
Butyl acrylate	300
Methyl methacrylate	300
Vinyl acetate	60
Sodium dioctyl sulfosuccinate	3
Potassium persulfate	2
Water	2380

Table 2. Recipe of the terpolymerization of BuA/MMA/VAc

Simulation-based Validation of the Moving-Horizon Observer

In order to apply the moving-horizon estimation scheme proposed in the preceding section to reconstruct the value of $N := (N_1, N_2, N_3)$ and μ, a constant evolution of μ is assumed (over the prediction horizon) and the general state equation is built up with the state vector being defined by :

$$x := \begin{pmatrix} N_1 & N_2 & N_3 & \mu \end{pmatrix} \in \mathbb{R}^4_+ \quad ; \quad \dot{\mu} = 0$$

Recall however that despite this constant behavior during the prediction horizon, the resulted *closed-loop* estimation of μ may show dynamic behavior thanks to the moving horizon technique (see figures 6 and 7).

Note that this is a concrete example of how dynamically unmodelled uncertain parameters can be tackled by the state extension technique that is described in section 2.1 [see equation (17)].

Considering global relative uncertainties d_1, d_2 and d_3, the following model is obtained to be used by the observer:

$$\dot{N} = \begin{pmatrix} 1+d_1 & 0 & 0 \\ 0 & 1+d_2 & 0 \\ 0 & 0 & 1+d_3 \end{pmatrix} \cdot f(x,u) \tag{39}$$

$$\dot{\mu} = 0 \tag{40}$$

$$y = (1+\nu) \cdot h(x) \tag{41}$$

Namely, relative uncertainties are introduced directly on the r.h.s of the system ODE's through the variables d_i's. This can gather all sources of model discrepancy. On the other hand measurement noises are introduced through the variable ν used in the measurement equation (41). More precisely, the following definitions of d and μ are used in the simulations:

$$d_i(k) = d_{max} \cdot r_i(k) \tag{42}$$

$$\nu(k) = \nu_{max} \cdot r_\nu(k) \tag{43}$$

where the $r_i(k)$'s and $\nu(k)$ are chosen randomly in $[-1, 1]$.

The results are shown on figures 2 and 3 (respectively without and in the presence of measurement noises) where up to 10% relative errors are introduced on the r.h.s of the system's model.

In order to show the benefit from the *singularity crossing* mechanism introduced in section 3, simulations with $N_{\text{trials}} = 1$ and $N_{\text{trials}} = 4$ are compared. The results are shown on Figure 4. The scenario being used is the same as the one depicted on figure 3.

Finally, to end this simulation based validation section, let us check the real time implementability of the moving-horizon observer. The computation times that lead to the results of figure 3 are given on Figure 5. Note that an explicit upper bound is imposed on the number of function evaluations. More precisely, the internal loop of the optimizer stops as soon as the computation time exceeds the sampling period (30 seconds). Note that all the results shown above use a tolerance threshold $\varepsilon = 10^{-8}$ for the optimization subroutine. It is shown in the following section illustrating the experimental validation results that this precision is unnecessarily high and quite similar results can be obtained using a lower precision (for instance $\varepsilon = 10^{-3}$) while reducing dramatically the computation time (see figures 6 and 7 hereafter). This is especially true under the multiple trials technique proposed above.

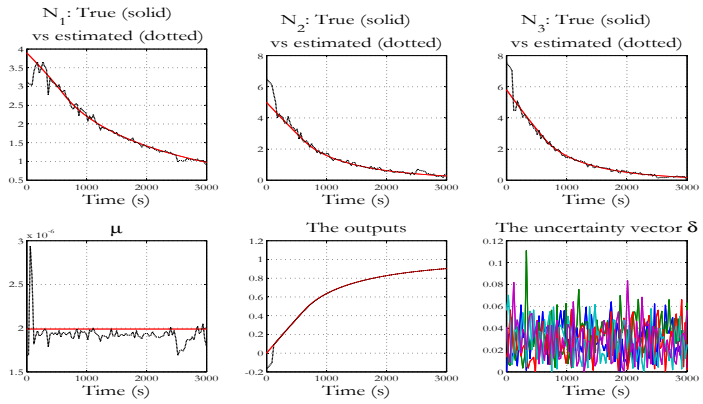

Fig. 2. *Observer behavior under model uncertainty given by (39)-(43) with* $d_{max} = 10\%$ *and no measurement noise* ($\nu_{max} = 0$). *The observation horizon is* $N = 10$ *and the number of trials for the singularity crossing scheme is* $N_{\text{trials}} = 4$. *Initial state of the observer is* $\hat{x}(0) = diag(0.8, 1.3, 1.3) \cdot x(0)$ *and* $\mu_{obs}(0) = 0.8\mu_{model}$.

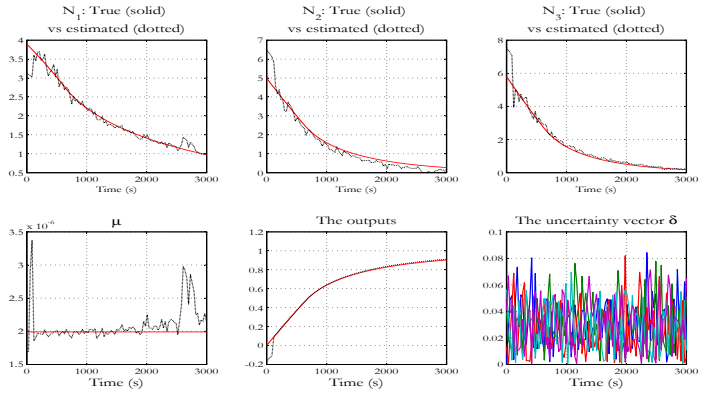

Fig. 3. *Observer behavior under model uncertainty given by (39)-(43) with* $d_{max} = 10\%$ *and in the presence of measurement noise* ($\nu_{max} = 0.01$). *The observation horizon is* $N = 15$ *and the number of trials for the singularity crossing scheme is* $N_{\text{trials}} = 4$. *Initial state of the observer is* $\hat{x}(0) = diag(0.8, 1.3, 1.3) \cdot x(0)$ *and* $\mu_{obs}(0) = 0.8\mu_{model}$. *Note that concerning the output, only the true output and the estimated one are shown, measurement noise is not presented. This scenario uses a tolerance* $\varepsilon = 10^{-8}$ *for the optimization subroutine.*

Experimental Validation of the Moving-Horizon Observer

In this section, the ability of the proposed state observer to reconstruct the individual values of N_1, N_2 and N_3 as well as the unmeasured and dynam-

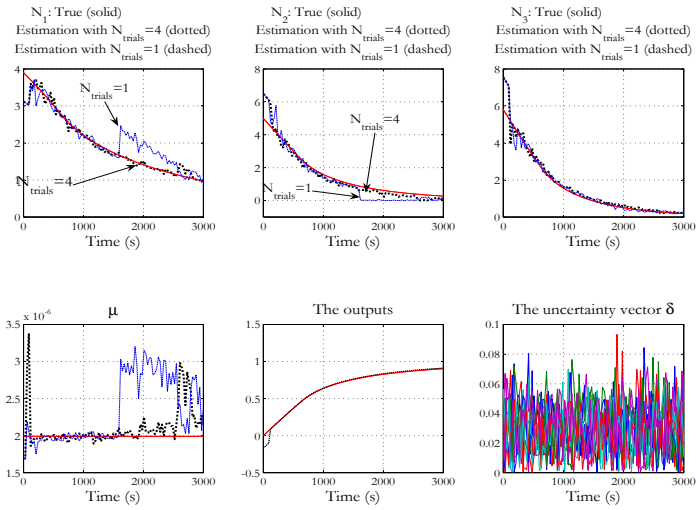

Fig. 4. *Comparison between the observer behavior when $N_{trials} = 1$ and $N_{trials} = 4$ under the scenario depicted on figure 3. Note how the singularity cross mechanism enables to avoid drops in the estimation quality when the observer encounters a singular situation. This scenario uses a tolerance $\varepsilon = 10^{-8}$ for the optimization subroutine.*

ically unmodeled variable μ is shown. Note that in order to experimentally measure the values of the N_i's, Samples are withdrawn during the reaction and an inhibitor is added to stop the reaction. The latex is then diluted in a solvent and injected in a gas chromatograph to measure the residual amount of monomer. By doing so, the true values of the N_i can be obtained. This has been done only during the 80 first minutes of the Batch where only 9 samples have been analyzed. The dots (*) on figures 6 and 7 indicate the corresponding measurements.

These figures clearly show the efficiency of the proposed pair (model,observer) in retrieving with an astonishing precision the values of the N_i's despite the unmodelled dynamic of μ. The rather short computation times (less than 5 seconds compared to the computation times obtained under high precision tolerance) underlines how real-time implementability depends on such parameters that are difficult to set a priori. Finally, it is worth underlying that the times needed to perform $N_{trials} = 10$ (figure 6) is much less than 10 times the mean computation time for $N_{trials} = 1$. This strengthens that the proposed singularity cross technique is different from the multiple initial guess technique in the sense that each trials starts from the best result achieved

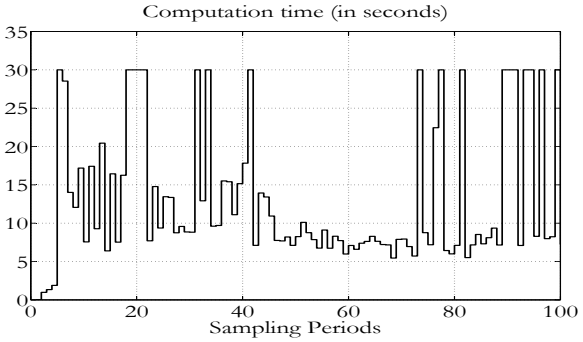

Fig. 5. *Computation times needed to achieve the state estimation depicted on figure 3. Note that an explicit upper bound has been imposed in the internal loop of the optimizer in order to deliver the best estimation that can be obtained within the available computation time defined by the sampling period (*30 *seconds). This scenario uses a tolerance* $\varepsilon = 10^{-8}$ *for the optimization subroutine.*

from the previous trial, only the weighting parameter vector $\bar{q}$ is randomly modified.

Figure 6 clearly shows an interesting (though expected) feature according to which the *closed-loop* dynamic of the additional state μ is much more *rich* than the dynamic used in the *prediction* algorithm. Indeed, while the supposed dynamic is $\dot{\mu} = 0$, the estimated evolution of μ shows realistic dynamic that is typical for this variable as it can be attested by polymerization experts. This asserts the efficiency of the *extended state* technique invoked in section 2.1 in handling the uncertainties using nominal uncertainty free framework even for uncertainties showing important dynamics.

4 Differential Form of Moving Horizon Observers

Throughout this section, the system model is assumed to be given in the following ODE form:

$$\dot{x}(t) = f(t, x(t)) \tag{44}$$

$$y(t) = h(t, x(t)) \tag{45}$$

This is because the differential form of the moving-horizon observer needs the time evolution of the system to be continuously differentiable. Consequently, under this assumption, there is no clear advantage from using the general form adopted in the preceding sections. The state and the output trajectories related notations, namely $X(t, t_0, x_0)$ and $Y(t, t_0, x_0)$ are however maintained

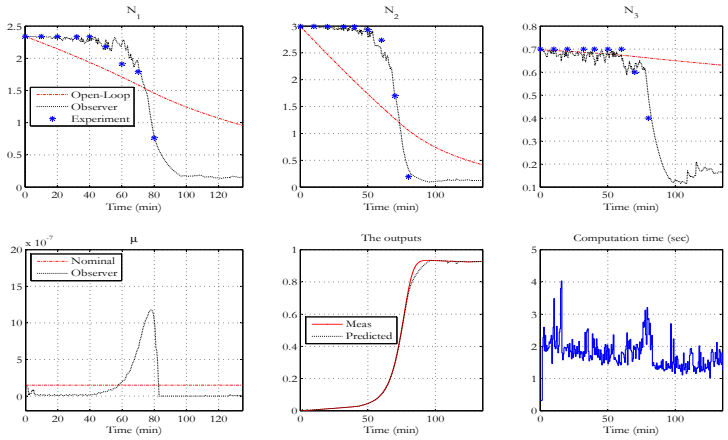

Fig. 6. *Experimental validation with $N_{trials} = 10$ and tolerance threshold $\varepsilon = 10^{-3}$ for the optimization subroutine. Note how the dynamic behavior of μ is recovered despite the constant behavior assumption used in the receding horizon observer model. The dashed lines show what would be obtained if an open-loop simulator is used to obtain an on-line estimation of the N_i's. Note the excellent matching between the experimentally measured values of the N_i's and those recovered by the observer. The same scenario is depicted on figure 7 where $N_{trials} = 1$ is used. Note also the quite rich estimated dynamic for μ despite the over simplified (constant) dynamic used in the definition of the extended state. This asserts the efficiency of using the extended state formalism in handling uncertainties using nominal uncertainty free framework.*

unchanged.

Throughout this section, it is assumed that the cost function $J(t, \xi(t))$ used in the receding-horizon estimation scheme is given by:

$$J(t, \xi) = \int_{t-T}^{t} \|Y(\tau, t-T, \xi) - y(\tau)\|^2 d\tau \tag{46}$$

In addition to the continuous differentiability of the r.h.s of (44), the following technical assumption is needed for the convergence result of the present section:

Assumption 1 (Uniform global regularity)
There is a **K-function** $\Upsilon : \mathbb{R}_+ \to \mathbb{R}_+$ *such that the following inequality holds:*

$$\|J_\xi(t, \xi)\|^2 \geq \Upsilon(J(t, \xi)) \tag{47}$$

for all (t, ξ) ♡

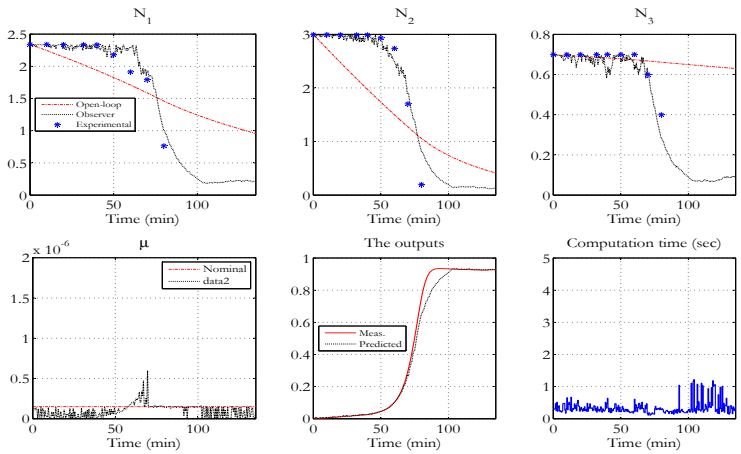

Fig. 7. *Results under the same experimental validation scenario as figure 6 with* $N_{trials} = 1$ *and tolerance threshold* $\varepsilon = 10^{-3}$. *Note the slight drop in the estimation quality (particularly on* N_2*) compared to figure 6 where the singularity cross technique is used.*

This assumption simply means that regardless the state $x(t-T)$ that holds at instant $t-T$, the corresponding cost function $J(t,\cdot)$ has a unique singular point which is precisely the unique global minimum $\xi = x(t-T)$. This is clearly a strong assumption that may not be necessary for the success of the estimation task in practical situations but that is mandatory to obtain a provably convergent state estimation scheme *in the large* (regardless the initial state estimation error). Locally, this property is clearly satisfied for systems (44)-(45) having an observable linearization (see [15] for more details). Further discussion on how to tackle the case where this assumption is not rigorously satisfied can be found in [13]. In this general survey on moving-horizon nonlinear observers, we restrict the presentation to the original basic framework. Another (although quite closely related) viewpoint leading to differential form of moving-horizon observer is based on continuation approach and can br found in [24]

The moving-horizon observer described in section 3 follows the standard scheme of the early formulation of [11] except that a singularities avoidance heuristic has been introduced. In particular, this formulation leaves aside the detailed description of the optimization process $\mathcal{S}$ used in (22) to perform the optimization task.

Regardless the particular choice of the optimizer $\mathcal{S}$, the classical scheme leads to a dynamic process on the observer's *internal state* $\xi(t)$ that is precisely

given by (28) which is reproduced here for clarity:

$$\begin{aligned}\xi(t_k) &= \mathcal{A}_{N_{\text{trials}}}\Big(\xi(t_{k-1}), t_k, y_{t_{k-N}}^{t_k}\Big)\\ \hat{x}(t_k) &= X(t_k, t_{k-N}, \xi(t_k))\end{aligned}$$

But there is clearly a more direct way to induce a dynamic on the internal state $\xi = \hat{x}(t-T)$ that is oriented towards the decrease of the cost function $J(t, \xi(t))$. Indeed, taking the time derivative of J, one may write[3]:

$$\dot{J}(t, \xi(t)) = J_t(t, \xi(t)) + \big[J_\xi(t, \xi(t))\big]\dot{\xi} \tag{48}$$

Note that the cost function $J(t, \xi(t))$ implicitly depends on the value of the state $x(t-T)$ at the past instant $t-T$. It is worth emphasizing however that this dependence involves only the past measurements y_{t-T}^{t} over the time interval $[t-T, t]$.

The evolution of ξ has to satisfy two conditions:

1. It must lead to a consistent observer in the absence of modeling errors and measurement noise. This means that if $\xi(t_0) = x(t_0 - T)$ at some instant t_0, then $\xi(t) = x(t-T)$ for all $t \geq t_0$. This implies the following *structure* for $\dot{\xi}$:

$$\dot{\xi}(t) = f(t-T, \xi(t)) + \underbrace{c(t, \xi(t))}_{\text{correction term}} . \tag{49}$$

   Note that the first term in the r.h.s of (49) is the nominal time derivative of $\xi(t)$ (i.e. when $\xi(t) = x(t-T)$) while $c(\cdot, \cdot)$ is a correction function that is such that:

$$\Big\{J(t, \xi(t)) = 0\Big\} \quad \Rightarrow \Big\{c(t, \xi(t)) = 0\Big\}.$$

   This enables to recover the nominal behavior as soon as $J(t, \xi(t)) = 0$, or equivalently as soon as $\xi(t) = x(t-T)$ under the observability condition in the sense of definition 3.

2. The correction term must be oriented towards the decrease of the cost function J.

Note that by injecting (49) in (48), the dynamic of J becomes:

$$\dot{J} = J_t(t, \xi(t)) + \Big[J_\xi(t, \xi(t))\Big] \cdot \Big[f(t-T, \xi(t)) + c\big(t, \xi(t)\big)\Big] \tag{50}$$

To go further, the following two lemmas are needed:

[3] Assuming that the necessary regularity conditions are satisfied

Lemma 1. *The correction-free time derivative of J satisfies:*

$$\frac{dJ}{dt}|_{c(\cdot,\cdot)\equiv 0} \leq |\epsilon_y(t,\xi(t)) - \epsilon_y(t-T,\xi(t))| + \Big[\phi(t,\xi(t))\Big] \cdot \sqrt{J}$$

where

$$\epsilon_y(\tau,\xi(t)) = Y(\tau,t-T,\xi(t)) - y(\tau) \quad \forall \tau \in [t-T,t]$$

♡

Proof *Taking the time derivative of (46) when no correction is used gives:*

$$\frac{dJ}{dt}|_{c(\cdot,\cdot)\equiv 0} = \epsilon_y(t,\xi(t)) - \epsilon_y(t-T,\xi(t)) + \tag{51}$$

$$\int_{t-T}^{t} \Big[Y(\tau,t-T,\xi(t)) - y(\tau)\Big]^T \Big[\tilde{\phi}(\tau,\xi(t))\Big] d\tau \tag{52}$$

where $\tilde{\phi}(t,\xi(t))$ is given by:

$$\tilde{\phi}(\tau,\xi(t)) := \frac{dY}{dt}\Big|_{c\equiv 0}(\tau,t-T,\xi(t)) - \dot{y}(\tau) \tag{53}$$

Using appropriate upper-bounding inequalities, equation (52) gives:

$$\frac{dJ}{dt}|_{c(\cdot,\cdot)\equiv 0} \leq |\epsilon_y(t,\xi(t)) - \epsilon_y(t-T,\xi(t))| + \tag{54}$$

$$\underbrace{\sup_{\tau\in[t-T,t]} \Big|\tilde{\phi}(\tau,\xi(t))\Big|}_{=:\phi(t,\xi(t))} \cdot \underbrace{\int_{t-T}^{t} \|Y(\tau,t-T,\xi(t)) - y(\tau)\|\, d\tau}_{\leq\sqrt{J}} \tag{55}$$

which clearly gives the result. □

Note that lemma 1 states that a function ϕ exists. The following lemma gives the conditions under which an upper bound i=of this function can be obtained to be used in the definition of the observer dynamic.

Lemma 2. *If it is possible to estimate an upper bound $\rho(t)$ satisfying:*

$$\forall \tau \in [t-T,t] \quad ; \quad \|\dot{y}(\tau)\| \leq \rho(t) \tag{56}$$

then there is a known computable function $\bar{\phi}_\rho(t,\xi(t))$ satisfying:

$$0 \leq \phi(t,\xi(t)) \leq \bar{\phi}_\rho(t,\xi(t)) \tag{57}$$

Proof This is a direct consequence of (53) from which it can be inferred that:

$$\phi(t,\xi(t)) \leq \sup_{\tau\in[t-T,t]} \Big[\|\frac{dY}{dt}\Big|_{c\equiv 0}(\tau,t-T,\xi(t))\| + \rho(t)\Big]$$

But for given τ, the time derivative of $Y(\tau, t-T, \xi(t))$ is given by:

$$\dot{Y}(\tau, t-T, \xi(t)) = Y_{t_2}(\tau, t-T, \xi(t)) + Y_\xi(\tau, t-T, \xi(t)) f(t-T, \xi(t))$$

where $Y_{t_2}(\cdot)$ is the partial derivative of Y w.r.t its second argument. The fact that the partial derivative terms Y_{t_2} and Y_ξ can be computed by classical sensitivity related ODE's ends the proof of the lemma. □

Based on lemmas 1 and 2, equation (50) leads to:

$$\dot{J} \leq \left|\Delta^t_{t-T}(\epsilon_y(\cdot, \xi(t)))\right| + \Big[\phi_\rho(t, \xi(t))\Big] \cdot \sqrt{J} + J_\xi(t, \xi(t)) \cdot c(t, \xi(t))$$

where the following short notation has been used:

$$\Delta^t_{t-T}(\epsilon_y(t, \xi(t))) = \epsilon_y(t, \xi(t)) - \epsilon_y(t-T, \xi(t))$$

This suggests the following expression for the correction term $c(t, \xi)$:

$$c(t, \xi(t)) := \gamma\Big[\frac{J_\xi^T(t, \xi(t))}{\|J_\xi\|^2 + \varepsilon}\Big]\Big[-\left|\Delta^t_{t-T}(\epsilon_y(\cdot, \xi(t)))\right| - \big[1 + \bar{\phi}_\rho(t, \xi(t))\big]\sqrt{J}\Big] \quad (58)$$

since when injecting this expression in (58), one obtains:

$$\dot{J}(t) \leq -\Big[\frac{\gamma\|J_\xi\|^2}{\|J_\xi\|^2 + \varepsilon} - 1\Big] \cdot \Big[\left|\Delta^t_{t-T}(\epsilon_y(\cdot, \xi(t)))\right| + \big[1 + \bar{\phi}_\rho(t, \xi(t))\big]\sqrt{J}\Big] \quad (59)$$

This means that as long as:

$$\|J_\xi(t, \xi(t))\|^2 > \frac{\varepsilon}{\gamma - 1} \quad (60)$$

the cost function J strictly decreases. Now using the inequality (47) with the above fact enables the following implication to be written:

$$\left\{\Upsilon(J(t, \xi(t)) > \frac{\varepsilon}{\gamma - 1}\right\} \quad \Rightarrow \quad \left\{\dot{J}(t, \xi(t)) < 0\right\}. \quad (61)$$

This clearly shows that under the correction law (58), the set defined by:

$$\mathcal{A}_J := \Big\{(t, \xi) \quad | \quad J(t, \xi) \leq \Upsilon^{-1}\Big(\frac{\varepsilon}{\gamma - 1}\Big)\Big\} \quad (62)$$

is an invariant and globally attractive set. But by the very definition of uniform observability (see definition 3), it can be inferred from (62) that the state estimation error $e = \xi(t) - x(t-T)$ satisfies the following asymptotic property:

$$\lim_{t \to \infty} \|\xi(t) - x(t-T)\| \leq \alpha^{-1} \circ \Upsilon^{-1}\Big(\frac{\varepsilon}{\gamma - 1}\Big) \quad (63)$$

and by continuity of the system trajectories w.r.t the initial state, property (63) clearly implies:

$$\lim_{(\varepsilon/\gamma)\to 0}\left[\lim_{t\to\infty}\|\hat{x}(t)-x(t)\|\right]=0. \tag{64}$$

The above discussion clearly proves the following result:

Proposition 1. *If the following conditions hold for the system (44)-(45):*

1. *The map f is continuously differentiable*
2. *The system is uniformly observable in the sense of definition 3*
3. *The uniform regularity assumption 1 is satisfied*
4. *It is possible to correctly estimate upper bounds of $y(\cdot)$ over past time intervals (see lemma 2)*

then for any a priori fixed desired precision $\eta>0$ on the state estimation error, there is a sufficiently high ratio γ/ε such that the dynamic system given by:

$$\dot{\xi}(t)=f(t-T,\xi(t))+c\big(t,\xi(t)\big) \tag{65}$$

$$\hat{x}(t)=X(t,t-T,\xi(t)) \tag{66}$$

where the correction term $c(t,\xi)$ is given by:

$$c(t,J):=\gamma\Big[\frac{J_\xi^T(t,\xi(t))}{\|J_\xi\|^2+\varepsilon}\Big]\Big[-\big|\Delta_{t-T}^t(\epsilon_y(\cdot,\xi(t)))\big|-\big[1+\bar{\phi}_\rho(t,\xi(t))\big]\sqrt{J}\Big] \tag{67}$$

leads to a state estimation error that asymptotically reaches the required precision η. ♡

It is worth noting that proposition 1 gives a receding-horizon observer that takes a rather classical form (differential equation built up with a correction term that is added to a copy of the system dynamic). There are two major differences however between this observer and classical analytic observers:

1. The first difference lies in the use of an integral norm J of the output prediction error in the correction term [see equation (67)] rather than its instantaneous value.

2. The second difference is the way the convergence is proved. While classical analytic observers investigate the evolution of the state estimation error which leads to the need for structural properties, here, the convergence proof is based on the convergence of J and this with the very definition of observability IMPLICITLY leads to the convergence of the state estimation error.

When compared to the classical moving-horizon observer scheme of section 3, the moving-horizon observer of proposition 1 contains apparently no optimization phase. Indeed, the optimization process is *embedded* in the dynamic of the internal state ξ. This dynamic

1. explicitly implements a gradient-based optimization process and
2. distribute the corresponding *iterations* over the system real life-time.

It is important to underline that the problem of local minima remains a common feature regardless the way the moving-horizon observer is implemented. In the context of proposition 1, this problem is hidden by the uniform global regularity assumption 1 (condition 3. of proposition 1). Note however that this assumption is not a constructive assumption in the sense that it is only needed for the convergence proof. The expression (67) of the observer dynamic is perfectly well defined even if this assumption is violated.

The real-time implementation of the observer equation (67) may face serious difficulties. This is because the computation of the gradient $J_\xi(t, \xi(t))$ is a quite involved task since it amounts to integrate a differential system of dimension $n(n+1)$ where n is the dimension of the state vector. This means that the time needed to perform the computation of the r.h.s of the observer equation, say τ_c can no more be neglected. This computation time represents naturally an upper bound on the sampling period $\tau_s (\geq \tau_c)$ that can be used to update the estimate of the state vector.

In the following section, a technical solution that is referred to as the post-stabilization technique is proposed in order to increase the sampling period while maintaining a good precision.

4.1 The post stabilization technique

In order to simplify the expressions, in this section, the observer equations (65)-(66) are shortly re-written in the following compact form:

$$\dot{\xi}(t) = f_c(t, \xi(t), J_\xi(t)) \tag{68}$$

$$\hat{x}(t) = X(t, t-T, \xi(t)) \tag{69}$$

Proposition 1 states that observing the state of the system amounts to *integrate* the differential system (68). According to the discussion of the end of the preceding section, this integration has to be done using relatively high sampling period τ_s. In order to efficiently integrate the differential system (68) despite this fact, it is important to note that this system satisfies the following *nice property*:

property

> The sub-manifold $J(t, \xi(t)) = 0$ is invariant under the combined dynamic of the system and the observer equations (18) and (68).

In [18], an efficient integration scheme has been proposed that is dedicated to differential systems having invariant sub-manifolds. This technique is roughly

depicted on figure 8. Namely, given the observer state $x(t_k)$ at instant $t_k = k\tau_s$, in order to obtain the next state $\xi(t_{k+1})$ at instant $t_{k+1} = (k+1)\tau_s$, the following steps are executed:

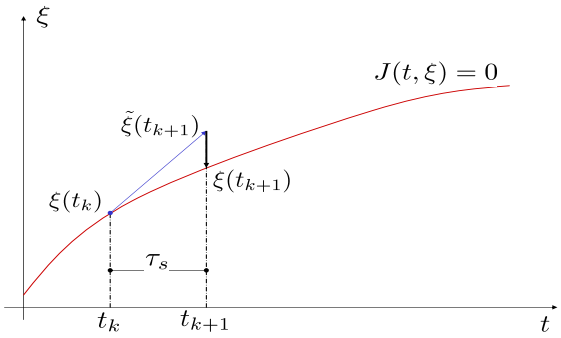

Fig. 8. The post-stabilization technique. To obtain the next observer state $\xi(t_{k+1})$, the observer equation is first integrated using constant gradient term $J_\xi(t_k, \xi(t_k))$, then the result $\tilde{\xi}(t_{k+1})$ is projected on the sub-manifold $J(t_{k+1}, \xi) = 0$.

✓ First, the following differential system is integrated over $[t_k, t_{k+1}]$ starting from the initial condition $(t_k, \xi(t_k))$:

$$\dot{\xi}(t) = f_c(t, \xi(t), J_\xi(t_k)) \quad ; \quad t \in [t_k, t_{k+1}] \tag{70}$$

The corresponding solution at instant t_{k+1} is denoted by $\tilde{\xi}(t_{k+1})$ (see figure 8). Note that during the integration over $[t_k, t_{k+1}]$, the gradient $J_\xi(t_k)$ is kept equal to its initial value at instant t_k. Consequently, $\tilde{\xi}(t_{k+1})$ is a rough approximation of the exact integration of the observer equation.

✓ The second step in the post stabilization technique is to correct the rough approximation $\tilde{\xi}(t_{k+1})$ by projecting it on the manifold $J(t_{k+1}, \xi) = 0$. This is written as follows:

$$\xi(t_{k+1}) = \tilde{\xi}(t_{k+1}) - \frac{J_\xi(t_{k+1}, \tilde{\xi}(t_{k+1}))}{\|J_\xi(t_{k+1}, \tilde{\xi}(t_{k+1}))\|^2 + \nu} \cdot J\big(t_{k+1}, \tilde{\xi}(t_{k+1})\big) \tag{71}$$

where $\nu > 0$ is a regularization constant that is used to avoid numerical singularities close to the surface.

A detailed investigation on the consequence of the above mentioned post-stabilization technique is presented in [15]. In particular, it has been shown

that when time invariant systems are considered the following asymptotic property holds:

$$\lim_{k\to\infty} J(\xi(t_k)) = O(\tau_s^4)$$

and this, regardless the order (≥ 1) of the integration scheme used to compute $\tilde{\xi}(t_{k+1})$.

4.2 Examples

In this section, two examples are given to illustrate the differential form of the moving-horizon observer presented in the preceding section. The first one (section 4.3) reports a successful industrial patented application [5] of this observer to the problem of the simultaneous estimation of the train velocity as well as the train position on a railways line. The second example (section 4.5) is a rather academic one that clearly shows the benefit from using the post-stabilization technique proposed in section 4.1 above. Another successful application of the differential moving-horizon observer can be found in [6] where this observation scheme has been applied to activated sludge processes used for waste-water treatment.

4.3 Nonlinear Observer for Tilting Trains

In this section, an industrial patented application [5] of the differential form of moving-horizon observer presented in this section is proposed[4]. The problem is first stated in the context of the control of tilting trains, then the need for an observer is explained and the performance of the proposed moving-horizon observer is shown.

Tilting trains: the control problem

The problem of controlling tilting trains is schematically depicted on figure 9. Typically, when the train goes into a bend of curvature $\rho(r)$ at some curvilinear abscissa r on the rails, a passenger feels a centrifugal acceleration $V^2\rho(r)$. This acceleration when combined with the gravity gives a resulting acceleration that is not perpendicular to the compartment floor unless the rails present a by-construction inclinaison $\delta(r)$.

Consequently, the rails are inclined in accordance with some *nominal* optimal velocity V_{nom} by an angle $\bar{\delta}(r)$ satisfying:

[4] This work has been achieved in a partnership context with the company ALSTOM-TRANSPORT (Villeurbanne, France). This partnership aimed to develop control algorithms for tilting trains. The work presented is described in details in the related patent [5]

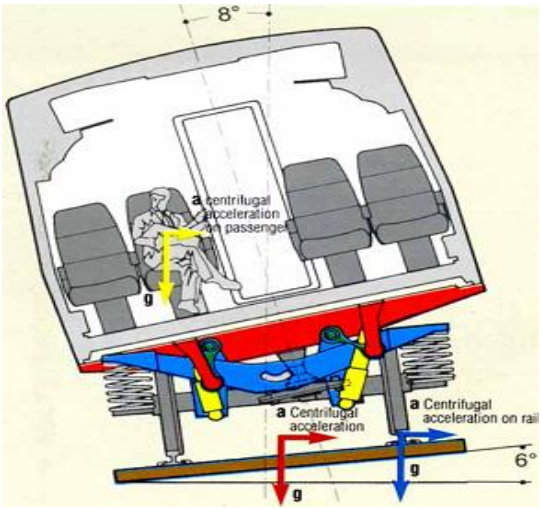

Fig. 9. Schematic view of a tilting train. The additional control-induced inclinaison of the compartment allows for a higher speed on existing rails while keeping the same comfort level (by maintaining the resulting felt acceleration normal to the compartment floor).

$$\bar{\delta}(r) = \tan^{-1}\Big(\frac{1}{g} \cdot V_{nom}^2 \cdot \rho(r)\Big) \tag{72}$$

Obviously, the curvature $\rho(\cdot)$ and the rails inclinaison $\delta(\cdot)$ become constant characteristics (profiles) of the rails. Now if the train follows these rails with a velocity that is significantly higher than the nominal velocity V_{nom} that has been used in the computation and the construction of the rails inclinaison profiles $\delta(\cdot)$, passenger would feel uncomfortable. The aim of the tilting train control is therefore to *compensate for the lack of rails inclinaison* by tilting the compartment using the dedicated jacks (see figure 9). Ideally, the additional inclinaison angle α_d is clearly given at instant t by:

$$\alpha_d(V(t), r(t)) := \tan^{-1}\Big(\frac{1}{g} \cdot V^2(t) \cdot \rho(r(t))\Big) - \bar{\delta}(r(t)) \tag{73}$$

Therefore, from a control point of view, the problem is to track a reference trajectory that depends on:

- The train's velocity $V(t)$
- The curvilinear abscissa of the train on the rails $r(t)$
- The geometric characteristics of the rails $\rho(\cdot)$ and $\bar{\delta}(\cdot)$

Remember that the origin of the control problem is related to the high velocities one aims to use that are higher than the nominal velocity V_{nom}. But the higher the velocity V is, the faster the set-point α_d changes since:

$$\dot{\alpha}_d = \frac{\partial \alpha_d}{\partial V}\dot{V} + \frac{\partial \alpha_d}{\partial r}V \approx \frac{\partial \alpha_d}{\partial r}(V, r)V \tag{74}$$

since the velocity of the train change slowly with time. This makes the tilting train control a very challenging problem that needs the use of advanced predictive control schemes enabling anticipating actions to be used. Indeed, a slight delay in the tracking may even give the inverse desired effect on the comfort level.

The estimation problem

Based on the above control problem description, it comes that anticipating the evolution of the desired set-point $\alpha_d(V(t), r(t))$ is a crucial issue. This means that the localization of the train on its rail is a key task in the overall control scheme. Note also that the estimation of a train velocity is a classical problem due to the need for a decentralized measurements for security reasons and due to the presence of slipping at the wheels level (see the patent [14] for more details on this critical issue).

Consequently, the estimation problem amounts to recover the evolution of both the curvilinear abscissa r and the error on the current estimation of the train velocity. To do this, the yaw angular velocity is available using a dedicated gyrometer that is fixed at the wheels level. Therefore, the dynamical system to be observed can be given as follows:

$$\dot{x}_1 = (1 + x_2) \cdot V_m(t) \tag{75}$$

$$\dot{x}_2 = 0 \tag{76}$$

$$y(t) = (1 + x_2(t))V_m(t) \cdot \rho(x_1(t)) \tag{77}$$

where $x_1 = r$ stands for the curvilinear abscissa of the train on the rail. x_2 is the relative error on the velocity, namely, the true velocity $V(t)$ is given by:

$$V(t) = (1 + x_2(t)) \cdot V_m(t)$$

The map $\rho(\cdot)$ is supposed to be available using dedicated series of measurements obtained during careful crossing of the line under consideration. The corresponding evolution of the curvature ρ as a function of the curvilinear abscissa is given on figure 10. This curve corresponds to the data characterizing a portion of the Paris-Toulouse line.

Note that in the above system model, the velocity measurement $V_m(\cdot)$ is supposed to be delivered by a dedicated velocity estimator or direct measurements. From the observation viewpoint, this signal is viewed as a known time varying signal over past intervals and can be handled using the estimation scheme through the time-varying character of the system model.

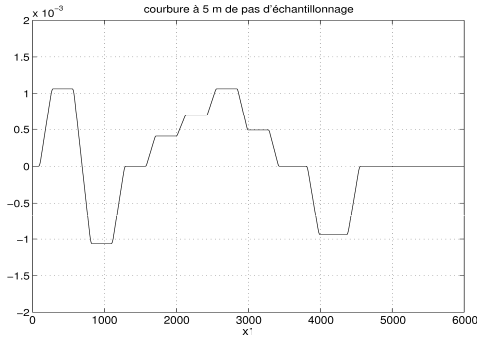

Fig. 10. Evolution of the curvature map $\rho(\cdot)$ on a portion of the Paris-Toulouse line. This map is used in the validating scenarios.

Based on the system model (75)-(77), the gradient $J_\xi(t,\xi)$ can be computed using the sensitivity matrix of the trajectory of the following system w.r.t initial conditions:

$$\begin{aligned}
\dot{z}_1 &= (1+z_2)V \\
\dot{z}_2 &= 0 \\
\dot{z}_3 &= \Big[(1+z_2)V\rho(z_1) - y\Big]^2
\end{aligned}$$

More precisely, one clearly has:

$$J_\xi(t,\xi) := \big(A_{31}(t)\ A_{32}(t)\big) \tag{78}$$

where the matrix $A(t) \in \mathbb{R}^{3\times 3}$ is the solution at instant t of the following differential system:

$$\dot{z}_1 = (1+z_2)V \tag{79}$$

$$\dot{z}_2 = 0 \qquad\qquad z(t-T) = \big(\xi^T\ 0\big)^T \tag{80}$$

$$\dot{z}_3 = \Big[(1+z_2)V\rho(z_1) - y(t)\Big]^2 \tag{81}$$

$$\dot{A}(\tau) = \begin{pmatrix} 0 & V(\tau) & 0 \\ 0 & 0 & 0 \\ \mathcal{X}_1(\tau) & \mathcal{X}_2(\tau) & 0 \end{pmatrix} A \quad ; \quad A(t-T) = \mathbb{I}_{3\times 3} \tag{82}$$

where the terms $\mathcal{X}_1$ and $\mathcal{X}_2$ are given by :

$$\begin{aligned}
\mathcal{X}_1 &= 2\Big[(1+z_2)V\cdot\rho(z_1) - y\Big](1+z_2)V\frac{\partial\rho}{\partial z_1}(z_1) \\
\mathcal{X}_2 &= 2\Big[(1+z_2)V\cdot\rho(z_1) - y\Big]\cdot V\cdot\rho(z_1)
\end{aligned}$$

Note that by integrating the differential system (79)-(82) over $[t-T, t]$ one obtains simultaneously $J_\xi(t, \xi(t))$ by (78) but also $J(t, \xi(t))$ by:

$$J(t, \xi(t)) = z_3(t).$$

Therefore, all that one needs to implement the differential moving horizon observer of proposition 1 can be obtained. It is worth noting that for this specific example, there is no need to integrate the 9th order differential system (79)-(82) since the structure of the system enables significant simplifications (see [5] for more details).

4.4 Simulations

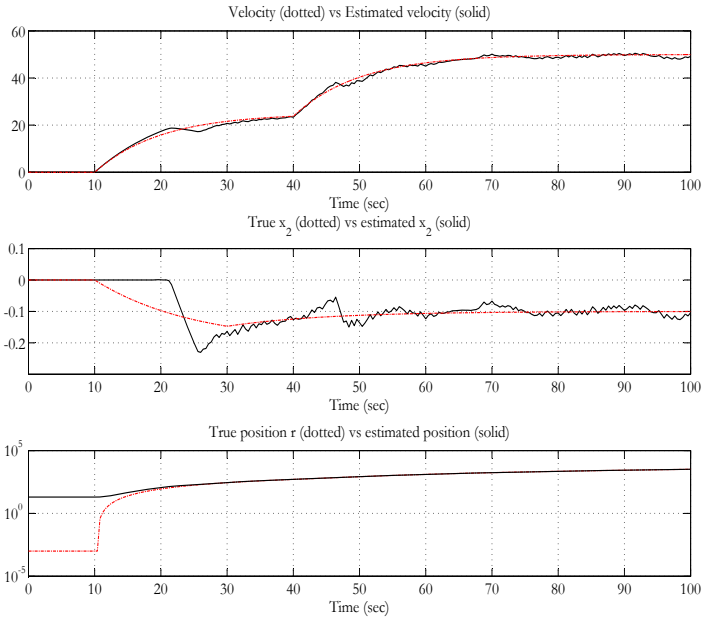

Fig. 11. Simulation of the differential moving-horizon observer when used to estimate the velocity and the position of a tilting train crossing a portion of the Paris-Toulouse line. Initial error on the position is equation de 20 m. The relative error on the velocity measurement varies form 0 to -15% during the first 20 seconds before it is settled to -10%. remember that the moving-horizon observer uses a constant evolution for this error when computing the cost function at each updating instant.

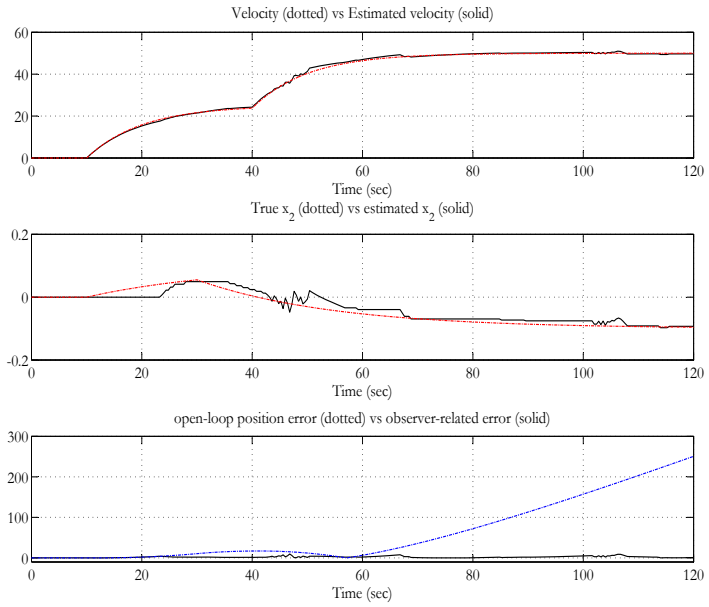

Fig. 12. Simulation of the differential moving-horizon observer when used to estimate the velocity and the position of a tilting train crossing a portion of the Paris-Toulouse line. Although there is no initial error on the position the bottom figure shows what would be the position error if no correction is made. The relative error on the velocity measurement varies form 0 to $+5\%$ and then to -10%. remember that the moving-horizon observer uses a constant evolution for this error when computing the cost function at each updating instant.

Simulations are conducted using the portion of the Paris-Toulouse line (see the corresponding curvature on figure 10) with the following parameters:

$$T = 5\ sec \quad ; \quad \tau_s = 0.4\ sec \quad ; \quad \gamma = 0.2$$

Two simulations are proposed to illustrate the benefit from using the proposed observer. In the first (figure 11), an initial error on the position is introduced as well as a time varying relative error on the velocity measurement. In the second scenario, a different profil on the velocity measurement error is used without initial error on the train position. Despite the absence of initial error, figure 12 shows what would be the error on the estimated position if the velocity measurement were integrated without correction. The consequence of using such erroneous position on the overall tilting control loop would be clearly dramatic.

4.5 Illustrating the benefit from using the post-stabilization step

The aim of this section is to illustrate how the post-stabilization step proposed in section 4.1 enables the updating period to be increased leaving more time for computations. This is done using the following academic example:

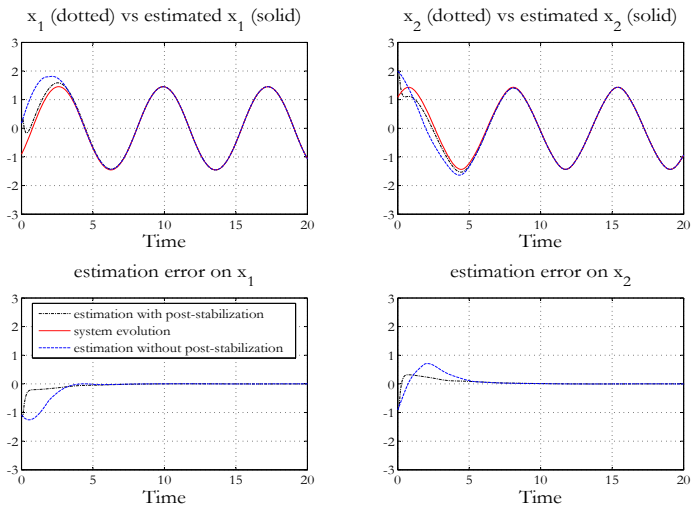

Fig. 13. Comparison between moving-horizon observer with (black dot-dashed line) and without (dotted) post-stabilization step. Here, the updating period is $\tau_s = 0.1\ s$. This si sufficiently small to make the moving-horizon observer stabilizing even without the post stabilization step. Even in this case, note how the post stabilization step improves the quality of the estimation.

$$\begin{aligned}\dot{x}_1 &= x_2\\ \dot{x}_2 &= -\sin(x_1) - 0.2x_1\cos(x_1x_2)\\ y &= x_1 + x_2\end{aligned}$$

Figures 13 and 14 show the behavior of the differential form of moving-horizon observer under two different updating periods $\tau_s = 0.1\ sec$ and $\tau_s = 0.4\ sec$.

When $\tau_s = 0.1\ sec$, the updating rate is sufficiently small for the observer to converge quite well even without the post stabilization step (see figure 13). However, when the updating period increases, the sampled observer fails to

converge without the post stabilization step (see figure 14).

It is worth noting that in both cases, it is the sampled version (70) of the differential moving-horizon observer that is implemented. This is precisely the reason for which a high updating period may destabilize the observer.

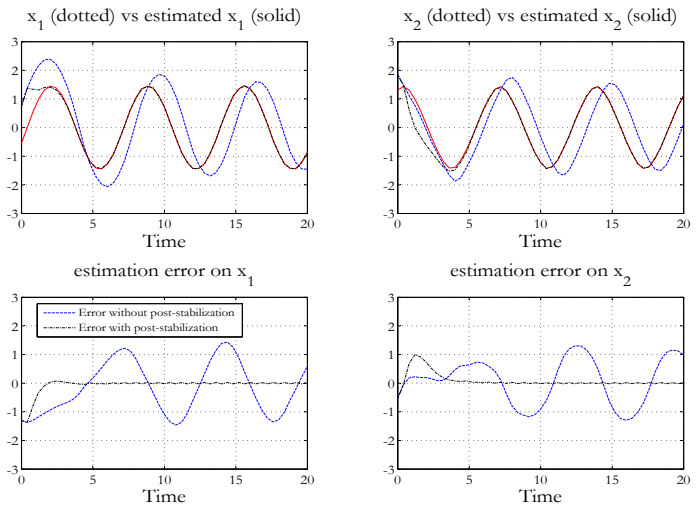

Fig. 14. Comparison between moving-horizon observer with (black dot-dashed line) and without (dotted) post-stabilization step. Here, the updating period is $\tau_s = 0.4\ s$. Note how the post stabilization step enables the updating period to be increased while maintaining good precision.

5 Moving Horizon Observers with Distributed Optimization

The differential form of the moving-horizon observer presented in section 4 tries to solve the optimization problem that underlines the state estimation problem using a gradient-based descent approach. Moreover, the iterations associated to this descent approach are distributed over the system life-time. The implementation of this approach needs however some regularity assumptions that guarantee the existence of all the partial derivatives of the cost function (the output prediction error).

In the present section, a more general viewpoint on the distributed-in-time

optimization is adopted in order to get deeper insight on the resulting closed-loop behavior. The ideas developed here are closely connected to those *in the air* when real-time implementation of Model Predictive Control is addressed (see for instance [16, 1, 9, 8]). The main message of this section is that even when efficient and globally convergent optimizers are used, there is some optimal updating rate of the internal state of the observer. This optimal sampling rate corresponds to some optimal number of iterations of the optimizer between two successive updates. It goes without saying that the quantitative translation of this general result heavily depends on the system, the optimizer and the computational facilities and should be approached using a somehow *experimental way*.

In this section, the general *simulator* form (1) of the dynamic system is considered, namely:

$$\begin{aligned} x(t) &= X(t, t_0, x_0), \\ y(t) &= h(t, x(t)), \end{aligned}$$

The measurement is assumed to be required with a sampling period τ_a. Note that τ_a defines the maximal frequency with which *additional new knowledge* is injected to any state estimation scheme. The acquisition period τ_a may be too small to be used as updating period[5] for the estimation. The updating period is considered here (without loss of generality) as a multiple of τ_a, namely, the updating period τ_u is defined by:

$$\tau_u = N_u \cdot \tau_a \quad \text{where } N_u \in \mathbb{N}$$

The resulting *updating instants* are therefore denoted by:

$$t_k = k \cdot \tau_u = k \cdot N_u \cdot \tau_a$$

The observation horizon T invoked in the above sections is here taken to be equal to an integer number N of acquisition periods, namely:

$$T := N \cdot \tau_a$$

that is, the observation horizon involves N past measurements. This enables the following cost function $J(t_k, \xi)$ to be defined at each updating instant t_k:

$$J(t_k, \xi) = \sum_{j=1}^{N} \Big\| Y(t_k - j\tau_a, t_k - T, \xi) - y(t_k - j\tau_a) \Big\|^2$$

Recall that minimizing $J(t_k, \xi)$ in the decision variable ξ amounts to look for the best estimate of the past state $x(t_k - T)$.

[5] The precise meaning of an updating period is made clear later on

Following the same notations than those used in section 3, we assume that some iterative process $\mathcal{S}$ has been chosen to minimize $J(t,\xi)$ in the decision variable ξ, namely:

$$\xi^{(i+1)} = \mathcal{S}\Big(t, \xi^{(i)}, y_{t-T}^{t}\Big)$$

The result of n successive application of $\mathcal{S}$ for given t is denoted by:

$$\xi^{(i+n)} = \mathcal{S}^{(n)}\Big(t, \xi^{(i)}, y_{t-T}^{t}\Big)$$

Let us consider the following assumption about the efficiency of the iterative process $\mathcal{S}$:

Assumption 2 [Efficiency of the optimizer]

Iterative process $\mathcal{S}$ is efficient in the sense that there exists some efficiency map $\alpha_{eff} : \mathbb{N} \to [0,1[$ such that for all t and ξ, one has:

$$J\Big(t, \mathcal{S}^{(n)}(t, \xi, y_{t-T}^{t})\Big) \leq \alpha_{eff}(n) \cdot J(t,\xi) \tag{83}$$

where $\alpha(\cdot)$ is a decreasing function such that $\alpha(0) = 1$. ♡

The state estimation algorithm studied in this section is defined by the following rules (see figure 15):

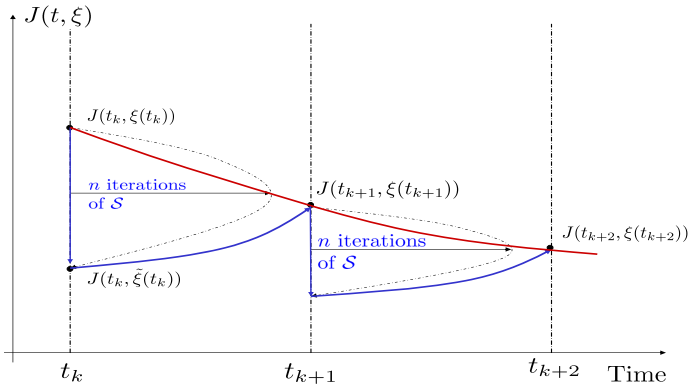

Fig. 15. Schematic view of the distributed-in-time optimization based observer. Note that the convergence of the overall estimation scheme is the result of a competition between a decreasing effect due to the optimizer and the increasing effect due to the natural divergence of open-loop state estimation.

(1) **Initial conditions**. Given that the estimation is based on past measurements over some prediction horizon $T = N \cdot \tau_a$. The estimation begins as soon as N measurements have been acquired. Consider some integer $k = k_0$ such that $k_0 \cdot N_u > N$. Assume that the current estimation of ξ is $\xi(t_k)$.

(2) **Updating** ξ. The computation of $\xi(t_{k+1})$ is done in two steps:

1. First n successive iterations are performed using the optimization process $\mathcal{S}$ to decrease the value of the cost function $J(t_k, \xi)$. This is written as follows

$$\tilde{\xi}(t_k) = \mathcal{S}^n(t_k, \xi(t_k), y_{t_k-T}^{t_k}) \tag{84}$$

Note that according to the assumption (83) on the optimizer's efficiency, one can write the following inequality:

$$J(t_k, \tilde{\xi}(t_k)) \leq \alpha_{eff}(n) \cdot J(t_k, \xi(t_k)) \tag{85}$$

2. Then the estimated value of $\xi(t_{k+1})$ is derived from $\tilde{\xi}(t_k)$ by integrating the system model:

$$\xi(t_{k+1}) = X(t_{k+1} - T, t_k - T, \tilde{\xi}(t_k)) \tag{86}$$

Note that when performing this *open-loop* updating over a time period of $N_u\tau_a = t_{k+1} - t_k$, some increase in the cost function have to be expected in general, this is stated by the following assumption:

Assumption 3 [open-loop behavior of the cost function]

When using open-loop prediction, the only inequality one can guarantee is given by:

$$J(t + \tau, X(t + \tau - T, t - T, \xi)) \leq \Big[J(t, \xi)\Big] \cdot \vartheta(\tau) \tag{87}$$

♡

using the inequality (87) with the following correspondances:

$$\xi = \tilde{\xi}(t_k) \quad ; \quad t = t_k \quad ; \quad \tau = N_u \cdot \tau_a$$

together with (86) enables to infer that when using the above estimation scheme, the inequality one can be sure of is the following:

$$J(t_{k+1}, \xi(t_{k+1})) \leq \Big[J(t_k, \tilde{\xi}(t_k))\Big] \cdot \vartheta(N_u\tau_a) \tag{88}$$

This with (85) enables the following inequality to be derived:

$$J(t_{k+1}, \xi(t_{k+1})) \leq \Big[\alpha_{eff}(n) \cdot \vartheta(N_u \tau_a)\Big] \cdot J(t_k, \xi(t_k)) \tag{89}$$

Note that the number of iterations n that may be performed during $N_u \tau_s$ time units is given by

$$n = E\Big(\frac{N_u \cdot \tau_a}{\tau_{iter}}\Big)$$

where τ_{iter} is the time needed for a single iteration.

Based on the above discussion, the following proposition can be derived:

Proposition 2. [Convergence of the distributed in time optimization based observers]

Under assumptions 2 and 3, the convergence of the distributed in time optimization based observer is guaranteed provided that the following inequality holds:

$$\varpi(N_u) := \alpha_{eff}\Big(E(\frac{N_u \tau_a}{\tau_{iter}})\Big) \cdot \vartheta(N_u \tau_a) < 1 \tag{90}$$

where

- ✓ τ_a *is the measurement acquisition period*
- ✓ $N_u \tau_a$ *is the updating period*
- ✓ τ_{iter} *is the time necessary to perform one iteration of the process* $\mathcal{S}$
- ✓ $\alpha_{eff}(\cdot)$ *is the optimizer efficiency map (see assumption 2)*
- ✓ $\vartheta(\cdot)$ *is the map characterizing the worst-case divergence rate of the open-loop prediction (see assumption 3)* ♠

Note that while condition (90) guarantees the convergence of the state estimation error. The corresponding *convergence time* (defined as the time needed for J to reach a value that is equal to 5% of its initial value) is still dependent on the value of N_u according to:

$$t_r(N_u) \approx \Big\lceil \frac{3N_u}{|\log\Big(\varpi(N_u)\Big)|} \Big\rceil \cdot \tau_a \tag{91}$$

It goes without saying that the exact expressions of the auxiliary functions $\alpha_{eff}(\cdot)$ and $\vartheta(\cdot)$ heavily depend on the system and the optimizer involved in the estimation scheme. however, in order to have concrete example showing the implication of the context on the *best* implementation parameters of the distributed-in-time optimization based state observers, let us consider the following structures for $\alpha_{eff}(\cdot)$ and $\vartheta(\cdot)$:

$$\alpha_{eff}(n) = \frac{D}{n^d + D} \quad ; \quad \vartheta(\tau) = \exp(\beta \cdot \tau) \tag{92}$$

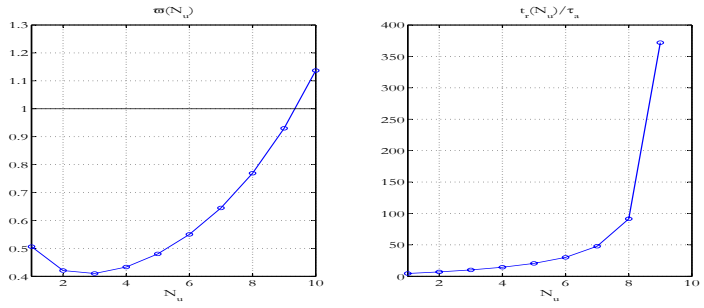

Fig. 16. Evolutions of the stability indicator $\varpi(N_u)$ and the settling time $t_r(N_u)$ vs the number of iterations N_u used to update the state estimation. The expressions (92) are used with the parameters $D = 3$, $d = 1$, $\beta \cdot \tau_a = 0.3$ and $\tau_a/\tau_{iter} = 5$. Under these conditions, stability cannot be guaranteed when more that 9 iterations are used. The optimal choice (in term of settling time) is the one where only one iteration is used to perform the updating.

Figures 16 and 17 give the evolution of the stability indicator ϖ and the settling time t_r as functions of the number of iterations N_u used to perform the observer internal state updating for two different sets of parameters used in (92). In the first case (figure 16), the instability rate of the open-loop estimation is high ($\beta \cdot \tau_a = 0.3$) leading to a maximum number of 9 iterations beyond which stability cannot be guaranteed. Moreover, the optimal choice in term of settling time is to use one single iteration before updating.

In the second case (figure 17), the instability rate is lower ($\beta \cdot \tau_a = 0.05$) and the efficiency of the iterations is higher ($d = 2$ rather than 1 in the first case). This leads to the stability being guaranteed for all number of iterations but with the optimal settling time corresponding to the use of 3 iterations.

6 Conclusion

The use of moving-horizon observers is intimately linked to the progress of nonlinear constrained optimization. However, the state estimation problem is not only an optimization problem. The way an optimization process can be used to result in a dynamic state estimator is to be carefully studied following (at least partially) some of the guidelines given in this chapter.

Another likely to be promising direction is to combine the partial use of analytic observer (on a part of the estimation problem) with the use of optimiza-

tion process. This enables optimization to concentrate on those parts of the problem where no particular structural properties are available.

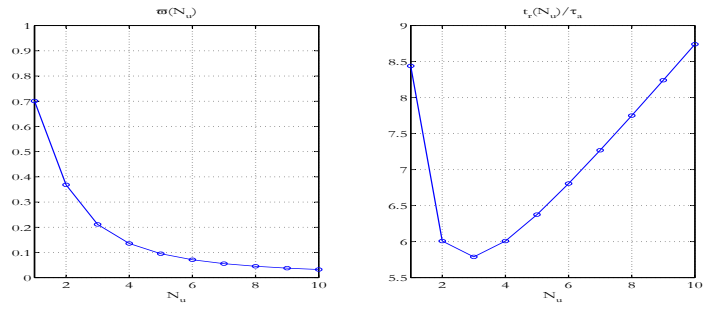

Fig. 17. Evolutions of the stability indicator $\varpi(N_u)$ and the settling time $t_r(N_u)$ vs the number of iterations N_u used to update the state estimation. The expressions (92) are used with the parameters $D = 50$, $d = 2$, $\beta \cdot \tau_a = 0.05$ and $\tau_a/\tau_{iter} = 5$. Under these conditions, while stability of the state estimation error seems guaranteed regardless the number of iterations used to perform the updating, the use of 3 iterations gives the best choice in term of settling time.

References

1. Alvarado I. A., Findeisen R., Kuhl P., Allgower F., and Limon D. State estimation for repetitive processes using iteratively improving moving horizon observers. In *Proceedings of the IFAC World Congress*, Barcelona, Spain, 2002.
2. Tornambè A. High gains observers for nonlinear systems. International Journal of Systems Science, 23, 1992.
3. Rao C. V.; Rawlings J. B. and Mayne D. Q. Constrained state estimation for nonlinear discrete-time systems: Stability and moving horizon approximation. *IEEE Transactions on Automatic Control*, 48(2):246–258, 2003.
4. Wang G. B., Peng S. S., and Huang H. A sliding observer for nonlinear process control. Chemical Engineering Science, 52, 1997.
5. Alacoque J. C. and Alamir M. Method and device for locating a vehicle on a road. Patent EP1211152, Alstom-Transport, http://gauss.ffii.org/PatentView/EP1211152, 2002.
6. Bassompierre C., Li S., and cadet C. Activated sludge processes state estimation: A nonlinear moving horizon observer approach. In *Proceedings of the American Control Conference*, Minneapolis, Minnesota, USA, 2006.
7. Kiparissides C., Seferlis P., Mourikas G., and Morris A.J. Online optimization control of molecular weight properties in batch free-radical polymerization reactors. Industrial Engineering and Chemistry Research, 41, 2002.

8. M. Diehl, R. Findeisen, and F. Allgöwer. A stabilizing real-time implementation of nonlinear model predictive control. In L. Biegler, O. Ghattas, M. Heinkenschloss, D. Keyes, and B. van Bloem Wanders, editors, *Real-Time PDE Optimization*, New York, 2006. Springer-Verlag. To appear.
9. M. Diehl, R. Findeisen, Z. Nagy, H.G. Bock, J.P. Schlöder, and F. Allgöwer. Real-time optimization and nonlinear model predictive control of processes governed by differential-algebraic equations. *J. Proc. Contr.*, 4(12):577–585, 2002.
10. Slotine J. E., Hedrick J. K., and Misawa E. A. On sliding observers for nonlinear systems. Journal of Dynamics Sysytems, Measurements and Control, 109, 1987.
11. Michalska H. and Mayne D. Q. Moving-horizon observers and observer-based control. *IEEE Transactions on Automatic Control*, 40:995–1006, 1995.
12. Buruaga I.S., Leiza J.R., and Asua J.M. Model-based control of emulsion terpolymerization based on calorimetric measurements. Polymer Reaction Engineering, 8(1), 2000.
13. Calvillo-Corona L. and Alamir M. Towards the construction of robust optimal observers. In *Proceedings of the IFAC World Congress*, Barcelona, Spain, 2002.
14. Thomas J. L., Latteux P., Alacoque J. C., Bornard G., and Alamir M. Method for estimating the velocity of a vehicle or an assembly of vehicles. Patent EP919814, Alcatel-Alstom Recherche, http://gauss.ffii.org/PatentView/EP919814, 2002.
15. Alamir M. Optimization based nonlinear observers revisited. *International Journal of Control*, 72 (13):1204–1217, 1999.
16. Alamir M. *Stabilization of Nonlinear Systems Using Receding-Horizon Control Schemes: A Parametrized Approach for Fast Systems.* Lecture Notes in Control and Information Sciences, Springer. Springer-Verlag, London, 2006.
17. Alamir M., Sheibat-Othman N., and Othman S. On the use of nonlinear receding-horizon observers in batch terpolymerization processes. Submitted to International Journal of Modelling, Identification and Control, 2007.
18. Ascher U. M. Stabilization of invariants of discretized differential systems. *Numerical Algorithms*, 14:1–24, 1997.
19. Othman N., McKenna T.F., and Févotte G. On-line monitoring of emulsion terpolymerization processes. Polymer Reaction Engineering, 9(4), 2001.
20. Gauthier J. P., Hammouri H., and Othman S. A simple observer for nonlinear systems – application to bio-reactors. IEEE Transactions on Automatic Control, 37, 1992.
21. Aguilar-Lopez R. and Maya-Yescas R. State estimation for nonlinear systems under model uncertainties: a class of sliding-mode observers. Journal of Process Control, 15, 2005.
22. BenAmor S., Doyle F.J., and McFarlane R. Polymer grade transition control using advanced real-time optimization sofware. Journal of Process Control, 14, 2004.
23. Ahmed-Ali T. and Lamnhabi-Lagarrigue F. Sliding observer-controller design for uncertain triangular nonlinear systems. IEEE Transactions on Automatic Control, 44(6), 1999.
24. Ohtsuka T. and Fujii H. A. Nonlinear receding horizon state estimation by realtime optiization technique. *J. Guidance, Control, Dynamics*, 19 (4):863–870, 1996.